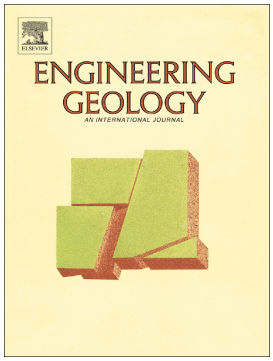

A mechanistic model for anisotropic thermal strain behavior of soft mudrocks

Biao Li, Ron C.K. Wong

PII: S0013-7952(17)30616-6
DOI: doi: 10.1016/j.enggeo.2017.08.008
Reference: ENGEO 4617

To appear in: *Engineering Geology*

Received date: 19 April 2017
Revised date: 1 August 2017
Accepted date: 3 August 2017

Please cite this article as: Biao Li, Ron C.K. Wong , A mechanistic model for anisotropic thermal strain behavior of soft mudrocks. The address for the corresponding author was captured as affiliation for all authors. Please check if appropriate. Engeo(2017), doi: 10.1016/j.enggeo.2017.08.008

A mechanistic model for anisotropic thermal strain behavior of soft mudrocks

by

Biao Li*

Department of Building, Civil & Environmental Engineering

Concordia University, Montreal, Quebec, Canada

Email: biao.li@concordia.ca

Complete mailing address: 1455 de Maisonneuve Blvd, W., EV6.166 Montreal, QC, Canada, H3G 1M8

(*corresponding author)

Ron C.K. Wong

Department of Civil Engineering, Schulich School of Engineering

University of Calgary, Calgary, Alberta, Canada

Email: rckwong@ucalgary.ca

Complete mailing address: Department of Civil Engineering, 2500 University Drive NW

Calgary, Alberta, Canada, T2N 1N4

(Submitted for publication 2017)

ABSTRACT

Under drained heating, soft mudrocks can expand or contract depending on its mineralogy, composition, structure, stress history, and the imposed temperature. Previous research on the physics behind the thermally induced deformation behavior is limited. The impact of clay minerals on the overall anisotropic deformation behavior has not been quantitatively considered. In this study, a compositional thermal strain model is proposed to quantify the thermally induced deformation in soft mudrocks through a homogenization approach. The intrinsic fabric of soft mudrock was examined and considered in the model. Theoretically, thermally induced deformation in a soft mudrock is contributed by the expansion of solid minerals and interlayer bound water, the removal or dehydration of clay-bound water, and thermal plastic strain (grain rearrangement). The overall deformation of soft mudrocks is governed by the thermal deformation behavior of individual constituents and their interactions. The interactions among non-clay minerals and clay-water composites can be considered by applying a structural state coefficient. The proposed thermal strain model was validated by a series of experimental results using reconstituted and natural soft mudrock samples with different clay fractions. The results indicate that soft mudrocks with a structural state of clay matrix-supported are on the risk of having thermal contraction behavior which comes from clay dehydration or thermal plastic strain. The oriented fabric in soft mudrocks contributes to the anisotropy in thermal strains. The proposed thermal strain model can be applied to estimate critical parameters in phenomenon-based thermal elastic-plastic models for constitutive modeling.

Keywords: Soft mudrock, microstructure, thermal strain model, anisotropy, mechanisms, experimental validation

1. Introduction

Soft mudrocks are usually shallowly buried and rich in swelling clay minerals. Thermally induced deformation in soft mudrocks may pose severe issues to thermal projects such as thermal heavy oil recovery and radioactive waste disposal (Hueckel and Baldi 1990; Jia et al. 2009; Sultan et al. 2002). Extensive experimental and theoretical work has been carried out on the thermal strain behavior of soft mudrocks or clay soils. Campanella and Mitchell (1968) concluded that heating can decrease the volume of normally consolidated clay specimens as long as full drainage is permitted and effective stresses are kept constant. More attention has been focused on the thermally induced deformation behavior of overconsolidated clay soils or soft mudrocks under drained stress path condition (Abuel-Naga et al. 2007; Hueckel and Baldi 1990). Overconsolidated soils or soft mudrocks with low over consolidation ratio (OCR) generally exhibit contractive thermal plastic behavior. With increasing OCR, the thermal plastic strains may be expansive (Abuel-Naga et al. 2007; Del Olmo et al. 1996; Di Donna and Laloui 2015; Sultan et al. 2002). Theoretical models have been proposed to match the laboratory measured thermal-mechanical behavior of clay-related geomaterials (Di Donna and Laloui 2015; Laloui and Cekerevac 2008; Hueckel and Baldi 1990). Generally, those theoretical models applied thermal elastic and plastic theories to account for reversible and irreversible strains, respectively. Little attentions have been focused on the physical mechanisms which can be used to interpret behaviors of anisotropy and thermal contraction due to the existence of clay minerals (Hueckel and Pellegrini 1996). Large amount of clay minerals presented in soft mudrocks have contributed to their complex micro-scale (inter-particle) and nano-scale (intra-particle) pores (Cariou et al. 2013; Li and Wong 2016). Amount of water molecules adhere to the clay mineral surface and form layers of clay-bound water, which takes up the nanoscale pore space. Geologists have

shown that the removal of clay-bound water (clay dehydration) at high temperature and pressure conditions would lead to contraction behavior of clay-related geomaterials (Colten-Bradley 1987; Vidal and Dubacq 2009). The thermal response of clay-bound water on overall thermal strain behavior of soft mudrocks was not well investigated in previous studies. The strain from clay dehydration was usually mixed with the component from thermal plastic strain (grain rearrangement). In addition, variations in the amount and type of clay minerals present in soft mudrocks or soils have contributed to their changes in compression behavior, swelling behavior, strength, permeability, fabric orientation distribution, and thermal conductivity (Barry-Macaulay et al. 2013; Day-Stirrat et al. 2011; Dewhurst et al. 1999; Ma et al. 2016). Those variations are quantitatively related to their structural states (Li and Wong 2016). Thus, clay fraction and structural state should also be considered in investigating mechanisms of anisotropic thermal strain behavior of soft mudrocks. Parameters in previous phenomenon-based thermal elastic-plastic models were obtained from complex thermal tests on soft mudrock samples which took a long time to finish. This is because a slow heating rate should have been applied to maintain a full drainage condition. The obtained parameters are not applicable for a different soft mudrock sample which has a different clay fraction. In this study, the impact of clay minerals on the overall deformation behavior of soft mudrocks was studied using a compositional thermal strain model. Experimental data were used to validate the proposed model. The study aims to facilitate thermal strain estimation without requiring a large quantity of thermal strain measurements.

2. Composition and structural state of soft mudrocks

Soft mudrock does not have strong cementations among mineral particles so it is a typical low strength sedimentary rock (Folk 1980). Shown in Fig. 1a, water-saturated soft mudrocks are

composed of non-clay minerals, clay minerals, and water. Non-clay minerals are large particles containing solid minerals such as quartz, feldspars, and pyrite. Non-clay minerals do not easily have physical or chemical interactions with water. In contrast, clay minerals can interact significantly with water, and clay minerals and water are usually treated as clay-water composites (Moyano et al. 2012). Free water in the microscale pore space of a soft mudrock will interact with clay particles and generate diffuse double layers (DDLs) (Mitchell and Soga 2005). Those water molecules adhering to the clay mineral surface form layers of clay-bound water and take up the nano-scale pore space (Fig. 1a). Such bound water is abundant both in the external and internal surfaces of smectite mineral (Murray 2007). Under water saturated condition, the clay-bound water requires high temperature and special pressure conditions to be removed (Colten-Bradley 1987; Vidal and Dubacq 2009). The microstructure of clay-water composite (clay particles and pores containing free water in micro-scale) can be examined using the technique of scanning electron microscope (SEM), where the oriented fabric in the sample can be observed and quantified (Cholach and Schmitt 2006). Advanced techniques such as transmission electron microscopy (TEM) and high-resolution X-ray texture goniometry are required to show the nano-scale fabric of clay minerals (Day-Stirrat et al. 2012). The orientation of a specific clay platelet can be noticed at this level. The nano-scale space of smectite is associated with interlayer bound water. When fresh water enters the interlayer of smectite, more DDLs could be generated. Thus, geomaterials containing a high content of smectite minerals have a high swelling potential. Those layers of bound water are well arranged both on the internal and external surfaces of clay particles (Fig. 1a). Those layers of bound water have the similar oriented fabric with clay particles, so swelling or hydration of mudrocks displays similar transversely isotropic behavior as elastic properties (Wong et al. 2008; Wong and Wang 1997).

Characterizing the fabric orientation distribution of soft mudrocks can be achieved by conducting free swell tests on vertically drilled samples (Wong and Wang 1997). Assuming no fabric rearrangement occurs during swelling, the fabric orientation distribution could be related to the anisotropy in swelling strains. For simplicity, the normal vector to the surfaces of plate-like mineral particles can be characterized by the following continuous distribution density function $f(\theta^f)$ (Li and Wong 2016; Wong and Wang 1997).

$$f(\theta^f) = \frac{1}{4\pi\left(1-\cos\theta^f\right)} \tag{1}$$

where θ^f is the fabric angle which has a range of $0 < \theta^f \le \frac{\pi}{2}$. The fabric orientation distribution function must satisfy the condition that:

$$2\int_0^{2\pi}\int_0^{\theta^f} f(\theta^f)\sin\gamma\, d\gamma\, d\beta = 1 \tag{2}$$

where γ and β are the spherical coordinates defining the normal direction of a clay particle. The three-dimensional viewing of the simplified fabric orientation distribution function can be found at Li and Wong (2016). When $\theta^f<\pi/2$, $f(\theta^f)$ is characterized by parts of a sphere, and the normal directions of clay particles are oriented to such parts of a sphere. When $\theta^f=\pi/2$, $f(\theta^f)$ is characterized by a complete sphere, and the normal directions of clay particles have the same possibility in any direction. Thus, a low value of θ^f indicates strong anisotropy in the fabric orientation distribution, and a value of $\pi/2$ indicates an isotropic fabric orientation distribution. According to Li and Wong (2017), fabric angle parameter of soft mudrocks can be estimated readily using measured properties such as clay fraction and porosity data.

Non-clay minerals have a high stiffness and serve as a structural framework of mudrocks when they have a high volume fraction (Fig. 1b). While clay-water composites are quite compressible and occupy the void space among non-clay minerals, they serve as an in-fill matrix. With the

increase of volume fraction of clay-water composites in soft mudrocks, there is a transition in the structural state from the state of framework-supported (dominated by non-clay minerals) to the state of matrix-supported (dominated by clay-water composites) (Fig. 1b).

The total volume of a sample, V is given as:

$$V = V_c + V_w + V_{nc} \tag{3}$$

where V_w is the volume of water, V_c is the volume of solid clay minerals, and V_{nc} is the volume of non-clay minerals.

The volume of clay-water composites, V_{cw} is given by:

$$V_{cw} = V_c + V_w \tag{4}$$

The clay fraction by mass for the sample, c_f is expressed as:

$$c_f = \frac{m_c}{m_c + m_{nc}} = \frac{\rho_c V_c}{\rho_c V_c + \rho_{nc} V_{nc}} \tag{5}$$

where m_c is the mass of solid clay particles, m_{nc} is the mass of non-clay minerals, ρ_c is the density of solid clay minerals, and ρ_{nc} is the density of non-clay minerals.

The sample porosity, ϕ is given by:

$$\phi = \frac{V_w}{V} \tag{6}$$

The volume fraction of clay-water composites, f_{cw} is given by:

$$f_{cw} = \frac{V_{cw}}{V} \tag{7}$$

The void ratio of clay-water composites, e_{cw} is given by:

$$e_{cw} = \frac{V_w}{V_c} \tag{8}$$

Non-clay minerals in soft mudrocks are mainly composed of quartz or feldspar which have a comparable density with clay minerals, thus ρ_c and ρ_{nc} have comparable values. Assuming $\rho_c = \rho_{nc}$, f_{cw} and e_{cw} are derived as:

$$f_{cw} = c_f(1-\phi) + \phi \tag{9}$$

$$e_{cw} = \frac{e}{c_f} \tag{10}$$

where e is the void ratio of the bulk rock, which is defined by $\frac{V_w}{V_c + V_{nc}}$ and is related to porosity by $e = \frac{\phi}{1-\phi}$.

With the increase of volume fraction of clay-water composites, the structural state transition behavior from the state of framework-supported to the state of matrix-supported was quantified by a c_m-model in Eq. (11) which was proposed by Li and Wong (2016).

$$c_m = \frac{\tanh\left(\frac{f_{cw} - 0.65}{0.16}\right) + 1}{2} \tag{11}$$

The value of c_m tends to be zero at low values of f_{cw} for the state of framework-supported, and c_m tends to be around one at high values of f_{cw} for the state of matrix-supported. The decreases in shear strength and pore size as well as the increases in compressibility and anisotropy in fabric are quantitatively related to such transition by applying the proposed c_m-model (Li and Wong 2016). The concept of structural state was applied by Li and Wong (2015) to estimate the thermally induced deformation behavior of shallowly buried shales, however, the parameters in the c_m-model were short of experimental validations.

3. A compositional thermal strain model

Under drained heating, the thermal deformation of soft mudrock can be caused by the expansion of solid minerals and interlayer bound water, the removal or dehydration of clay-bound water, and thermal plastic strain (grain rearrangement) as expressed in Eq. (12)

$$d\varepsilon^{T} = d\varepsilon^{Te} + d\varepsilon^{Td} + d\varepsilon^{Tp} \tag{12}$$

where $d\varepsilon^{T}$ is the total thermally induced volumetric strain, $d\varepsilon^{Te}$ is the strain caused by thermal elastic deformation of solid minerals and interlayer bound water, $d\varepsilon^{Td}$ is the strain caused by clay dehydration, and $d\varepsilon^{Tp}$ is the thermal plastic strain. In this study, the strain of thermal expansion is treated as positive and the strain of thermal contraction is treated as negative. Since soft mudrocks have transversely isotropic oriented fabric, the deformations along the horizontal (x or y, $d\varepsilon_x^T$ or $d\varepsilon_y^T$), and vertical (z, $d\varepsilon_z^T$) directions of a sample are expressed as Eq. (13).

$$\begin{cases} d\varepsilon_x^T = d\varepsilon_x^{Te} + d\varepsilon_x^{Td} + d\varepsilon_x^{Tp}, d\varepsilon_y^T = d\varepsilon_x^T \\ d\varepsilon_z^T = d\varepsilon_z^{Te} + d\varepsilon_z^{Td} + d\varepsilon_z^{Tp} \end{cases} \tag{13}$$

The proposed compositional thermal strain model presents equivalent thermal deformation property of a soft mudrock based on the thermal deformation behavior of individual constituents and their volume fractions. Under heating, non-clay minerals are always expanding; however, clay-water composites may contract due to clay dehydration or thermal plastic strain. Clay dehydration mainly happens to the smectite mineral (Vidal and Dubacq 2009) and thermal plastic strain can happen to all the clay minerals (Hueckel and Baldi 1990; Di Donna and Laloui 2015). The structural state has very little impact on the thermal expansion of solid minerals and interlayer bound water since all constituents are contributing to the thermal expansion behavior of a mudrock. However, the contribution of contraction behavior caused by clay dehydration and thermal plastic strain in the thermal deformation behavior of soft mudrocks depends on the

structural state. When a sample belongs to the state of framework-supported, the contraction in clay-water composites has a limited effect on the overall deformation behavior of a mudrock sample. Instead, if the sample has a state of clay matrix-supported, the mudrock is percolated by clay-water composites and the contraction in clay-water composites certainly contributes to the overall deformation behavior. The proposed c_m-model was applied to take into account the interactions among non-clay minerals and clay-water composites when conducting homogenization for deformation components caused by clay dehydration and thermal plastic strain. It should be noted that the proposed theoretical model is only applicable for a soft mudrock or clay soil which has no strong crystal cementation among different minerals and the studied temperature is below 250°C. In some brittle rocks, thermally induced micro-crack will have an impact on the estimation of thermal expansion coefficients (Zhao et al. 2017), and the proposed homogenization approach will not be applicable.

3.1 Thermal elastic deformation of solid minerals and interlayer bound water

Both non-clay minerals and clay-water composites contribute to the thermal elastic deformation of a mudrock sample, and the amount of contribution depends on their volume fractions. Non-clay minerals have isotropic thermal expansion behavior upon heating. For clay-water composites, the thermal elastic deformation is governed by the clay skeleton which is composed of clay minerals and interlayer bound water. As shown in Fig. 2, both clay minerals and clay-bound water will expand upon heating. Interlayer bound water is in nano-scale pore space and requires special temperature, pressure, and time conditions to deplete, which will be discussed in detail in the next section. Clay-water composites can have anisotropic thermal expansion behaviors due to the oriented fabric. Anisotropic thermal elastic strains in a soft mudrock caused by thermal elastic deformation of solid minerals and interlayer bound water are expressed by:

$$\begin{cases} d\varepsilon_x^{Te} = \alpha_l^{nc}\Delta T\left(1-f_{cw}\right)+f_{cw}\left(\varepsilon_x^{c}\left(1-f_{ic}\right)+\varepsilon_x^{iw}f_{ic}\right) \\ d\varepsilon_z^{Te} = \alpha_l^{nc}\Delta T\left(1-f_{cw}\right)+f_{cw}\left(\varepsilon_z^{c}\left(1-f_{ic}\right)+\varepsilon_z^{iw}f_{ic}\right) \end{cases} \tag{14}$$

where α_l^{nc} is the linear thermal expansion coefficient of non-clay minerals, and ΔT is the temperature change; ε^c and ε^{iw} are thermal strains of solid clay minerals and interlayer bound water, and the subscript indicates for the strain along a specific direction such as x, y or z.

The volume fraction of interlayer water over a clay skeleton, f_{ic} can be given by:

$$f_{ic} = \frac{V_i}{V_i + V_c} \tag{15}$$

where V_i is the volume of interlayer water; V_c is the volume of solid clay mineral; $V_i + V_c$ is the volume of clay skeleton. According to some researchers (Colten-Bradley 1987; Vidal and Dubacq 2009), V_i has a comparable value (about 3/4) of the volume of smectite platelet. Given the volume fraction of smectite in clay minerals (f_{sc}), f_{ic} can be derived as:

$$f_{ic} = \frac{3f_{sc}}{3f_{sc}+4} \tag{16}$$

All non-cubic minerals such as quartz and those clay minerals have anisotropic thermal expansion coefficients (Skinner, 1966). However, non-clay minerals are mostly formed as granular particles, and their crystal axes are usually randomly arranged. For simplicity, we just assume that non-clay minerals have a linear isotropic thermal expansion coefficient, α_l^{inc}, which could be approximated by the averaged linear thermal expansion coefficients of quartz and feldspar since they are the dominant non-clay minerals. An average value of 11.3×10^{-6}/°C for the linear thermal expansion coefficient of quartz and feldspar was provided by Robertson (1988).

Thermal expansion coefficients of solid clay minerals have been investigated by McKinstr (1965) who concluded that most clay minerals have anisotropic thermal expansion behavior. Taking a clay mineral particle for example (Fig. 3), the direction perpendicular to the basal spacing is marked as direction 1 and the direction parallel to the platelet plane is marked as direction 2. Measured anisotropic thermal expansion coefficients (α_1^c for the direction 1, and α_2^c for the direction 2) of some common clay mineral platelets are included in Table 1. Muscovite and kaolinite have significant anisotropy in thermal expansion behavior, where α_1^c are much higher than α_2^c. Chlorite has comparable thermal expansion coefficients for α_1^c and α_2^c. For soft mudrocks which are rich in muscovite and kaolinite, average values for α_1^c and α_2^c are given as 18.2×10^{-6}/°C and 4.35×10^{-6}/°C, respectively. With the fabric distribution function described in Eq. (1), the thermal elastic strains of clay minerals along the x- and z- directions, ε_x^c and ε_z^c are derived as:

$$\begin{cases} \varepsilon_x^c = 8\int_0^{\frac{\pi}{2}}\int_0^{\theta^f}\left(\alpha_1^c \sin\gamma\cos\beta + \alpha_2^c \cos\gamma\cos\beta\right)\Delta T f(\theta^f)\sin\gamma d\gamma d\beta \\ \varepsilon_z^c = 8\int_0^{\frac{\pi}{2}}\int_0^{\theta^f}\left(\alpha_1^c \cos\gamma + \alpha_2^c \sin\gamma\right)\Delta T f(\theta^f)\sin\gamma d\gamma d\beta \end{cases} \tag{17}$$

Nano-scale interlayer bound water has different thermal expansion behavior when compared with free water. Thermal expansion behavior of water in pores about 50 Å in size has been investigated by Derjaguin et al. (1992). The nonlinear thermal strain, ε^{iw} of such bound water can be approximated by a function shown in Fig. 4. Interlayer bound water has the similar oriented fabric with the clay platelet. With the fabric distribution function described in Eq. (1), the thermal elastic strains of interlayer bound water along the x- and z- directions, ε_x^{iw} and ε_z^{iw} are derived as:

$$\begin{cases} \varepsilon_x^{iw} = 8\int_0^{\frac{\pi}{2}}\int_0^{\theta^f} \varepsilon^{iw} f(\theta^f)\sin\gamma\cos\beta\sin\gamma d\gamma d\beta \\ \varepsilon_z^{iw} = 8\int_0^{\frac{\pi}{2}}\int_0^{\theta^f} \varepsilon^{iw} f(\theta^f)\cos\gamma\sin\gamma d\gamma d\beta \end{cases} \tag{18}$$

3.2 The strain caused by clay dehydration

Soft mudrocks hold an amount of clay-bound water in the external and internal surfaces of clay minerals. Clay dehydration plays an important role in the process of thermally induced deformation of clay-related geomaterials (Colten-Bradley 1987; Hüpers and Kopf 2009; Vidal and Dubacq 2009). The increase in the energy of water molecules caused by heating results in the weakening of their bond with the mineral surface and transforming bound water into free water (Colten-Bradley, 1987). Fig. 5 illustrates a representative elementary volume (REV) of clay-water composites in a mudrock under an effective stress of σ' and pore pressure of p_f. The pore pressure within the clay bound water is marked as p_i. If a mudrock is heated to a temperature that all the clay-bound water turns to be free water, mobile water in the clay-water composite system of a mudrock could be drained out under stress and drained conditions as shown in Fig. 5. Previous researches indicate that the pore pressure within clay bound water, P_i is equal to the effective stress, σ' for heavily over consolidated clays or mudrocks (Gonçalvès et al. 2010; Zhang et al. 2012). As long as there is an effective stress, free water in the micro-space of a mudrock could be drained out through the micro-scale flow. However, water in the nano-space can only be drained out when $p_i > p_f$ ($\sigma' > p_f$), and it will take a long period to escape through nano-scale flow. Clay dehydration could contribute to the contraction of a mudrock depending on the structural state. The deformation behavior of a sample with a structural state of framework-supported might not be affected of clay dehydration, but the deformation behavior will be strongly affected by clay dehydration if the sample has a structural state of clay matrix-

supported. The proposed c_m-model was applied using a coefficient to account for the interactions among constituents of soft mudrocks. The thermally induced volumetric strain in shale due to clay dehydration can be derived as:

$$d\varepsilon^{Td} = c_m \frac{\Delta V^{Td}}{V} \tag{19}$$

where ΔV^{Td} is the volume of removed or dehydrated clay-bound water (negative indicates for contraction). ΔV^{Td} can be calculated by:

$$\Delta V^{Td} = -A_c \Delta d \tag{20}$$

where A_c is the surface area of clay minerals and Δd is the change in bound-water thickness caused by dehydration.

The surface area of clay minerals, A_c is given by:

$$A_c = m_c S_c \tag{21}$$

where S_c is the specific surface of clay minerals (m^2/g). If only the clay bound water stacked to the external surface of clay minerals is removed, the external specific surface area, S_c^e should be applied; If all the clay-bound water is able to be removed, the total specific surface area, S_c^t should be applied instead. The pore size for hydraulic flow along the external specific surface of soft mudrock is approximately 1 μm, and the pore size in the nano-space of smectite is less than 1 nm (Cariou et al., 2013). Assuming that flow conduits in soft mudrocks are composed of bundles of tubes, the drainage rate is governed mainly by the pore size, which is given by Poiseuille's law. For a given pressure drop per unit length, the volume rate of flow is inversely proportional to the viscosity and proportional to the tube radius raised to a power of four (Munson et al. 2002). The rate of flow through smectite interlayers is 12 orders of magnitude less than that in the micro-pore among particles. In addition, the viscosity of water in the smectite

interlayer is much lower than that of free water, which also leads to a low flow rate (Ichikawa and Selvadurai 2012). Thereby, total specific surface area, S_c^t will only be applied for studying on thermal behaviors under a very long period of heating. For most geomechanical laboratory tests, only a short period of time (days to weeks) is spent on the measurement, so the parameter of external specific surface area, S_c^e should be applied herein. Details on determining the parameter of S_c^e for soft mudrocks is included in the discussion section.

With equations (6), (7), (9), (19), (20) and (21), $d\varepsilon^{Td}$ is given by:

$$d\varepsilon^{Td} = -c_m \rho_c S_c (1-\phi) c_f \Delta d \tag{22}$$

The change in bound-water thickness, Δd, caused by clay dehydration, has been quantified by Colten-Bradley (1987), and Vidal and Dubacq (2009). High-pressure and high-temperature X-ray cells were used in their tests to determine the basal spacing of clay platelets from oriented mounts. With temperature increase, the three layers of bound water (Fig. 1a) will be depleted progressively. The result indicates that the removal of clay-bound water is reversible. The thickness of one layer of bound water is approximately 1.5 Å. The temperature of depleting the clay-bound water depends on the pressure condition and water activities. The measured results of the relationship between the change of bound-water thickness and temperature are presented in Fig. 6. The results of Colten-Bradley (1987) are based on Na-montmorillonite, and the results of Vidal and Dubacq (2009) are based on K-, Na-, Ca-, and Mg-smectite. In general, K- or Na-smectite requires lower temperature for clay dehydration than Ca- and Mg-smectite. An equation is proposed to approximate such a correlation, as shown in Eq. (23) and Fig. 6.

$$\Delta d = \begin{cases} 0, & T < 55 \\ 4.5(0.0069T - 0.3793), & 55 \le T \le 200 \\ 4.5, & T > 200 \end{cases} \tag{23}$$

where the unit of T is °C and the unit of Δd is Å.

The proposed compositional thermal strain model only deals with the thermal strain at a temperature belong 250°C and it has not taken into account mineral transformations in soft mudrocks. Some dehydration due to recrystallization at very high temperature (e.g., T >600°C) is beyond the scope of this study.

With the fabric distribution function described in Eq. (1), the strains due to clay dehydration along the x- and z- directions, $d\varepsilon_x^{Td}$ and $d\varepsilon_z^{Td}$ are derived as:

$$\begin{cases} d\varepsilon_x^{Td} = 8\int_0^{\frac{\pi}{2}}\int_0^{\theta^f} d\varepsilon^{Td} f(\theta^f)\sin\gamma\cos\beta\sin\gamma d\gamma d\beta \\ d\varepsilon_z^{Td} = 8\int_0^{\frac{\pi}{2}}\int_0^{\theta^f} d\varepsilon^{Td} f(\theta^f)\cos\gamma\sin\gamma d\gamma d\beta \end{cases} \tag{24}$$

3.3 Thermal plastic strain

Anisotropic expansion of clay platelets and the depletion of bound water could trigger rearrangement and structural changes in non-clay minerals and clay-water composites, which result in thermal plastic strain in a soft mudrock. Similar to the strain caused by clay dehydration, thermal plastic strain in a soft mudrock is also affected by the sample's structural state. Thus, the proposed c_m-model is also introduced herein. Thermal plastic strain, $d\varepsilon^{Tp}$ of the mudrock is given as:

$$d\varepsilon^{Tp} = c_m \frac{\Delta V^{Tp}}{V} \tag{25}$$

where ΔV^{Tp} is the volume change in the mudrock due to thermal plastic strain. It equals to the volume change in clay-water composites due to thermal plastic strain, ΔV_{cw}^{Tp}.

Based on Eqs. (7) and (8), $\frac{\Delta V^{Tp}}{V}$ is given by:

$$\frac{\Delta V^{Tp}}{V} = - f_{cw} \frac{\Delta e_{cw}^{Tp}}{1+e_{cw0}} \tag{26}$$

where Δe_{cw}^{Tp} is the change in void ratio of clay-water composites due to thermal plastic strain (positive indicates contraction), and e_{cw0} is the initial void ratio of clay-water composites.

Thermal consolidation which is contributed by clay dehydration and thermal plastic strain has been recognized in consolidation tests at various temperatures on clay soils (Campanella and Mitchell 1968; Hüpers and Kopf 2009). Those tests were conducted on fine-grained geomaterials with different clay mineralogy and compositions. The results indicate that the slope of the normally consolidation curve is independent of temperature but the consolidation curve shifts downward at higher temperatures. A sketch illustrating this phenomenon is shown in Fig. 7. Thermally induced void ratio change of a sample, Δe^{T} contains the component due to clay dehydration, Δe^{Td}, and the component of thermal plastic strain, Δe^{Tp}. The amount from clay dehydration is reversible under cooling but the amount from thermal plastic strain is irreversible. Thermal plastic strains, ε^{Tp} or void ratio changes due to thermal plastic deformation, Δe^{Tp} of some fine-grained geomaterials were measured by several researchers based on heating and cooling tests under normally consolidated stress condition. Petrophysical properties and measured thermal plastic strain results of those geomaterials are included in Table 2. Samples range from smectite-rich Marine clay and Bangkok clay (Demars and Charles 1982) to pure kaolinite (Laloui and Cekerevac 2008) and all samples have high clay fractions (c_m close to 1). Among those properties, Δe_{cw}^{Tp} was derived from measured ε^{Tp} or Δe^{Tp} based on Eq. (25). Data of Δe_{cw}^{Tp} was plotted against temperature in Fig. 8. At the same temperature, kaolinite and Bangkok clay correspond to the lower and upper bounds of Δe_{cw}^{Tp}, respectively. As a typical soft

mudrock, a general trend for the correlation between Δe_{cw}^{Tp} and T of Boom clay mudstone can be found as shown in Fig. 9. A model similar to that of clay dehydration given in Eq. (27) was proposed to quantify Δe_{cw}^{Tp} as a function of temperature (shown in Fig. 9 and Eq. (27)):

$$\Delta e_{cw}^{Tp} = \begin{cases} 0, & T < 22 \\ 0.13\left(0.0056T - 0.1236\right) & 22 \le T \le 200 \\ 0.13 & T > 200 \end{cases} \tag{27}$$

where the unit of T is °C.

In contrast to clay dehydration which initiates at a temperature higher than 50°C, thermal plastic deformation starts from the beginning of heating. It is because an anisotropic expansion of solid clay platelets occurs upon heating and it can result in grain rearrangement (Fig. 2).

When a soft mudrock is not under a normally consolidated stress state, the effect of stress history on thermal plastic strain should be considered. The effect of stress history on thermal plastic strain of fine-grained geomaterials has been studied by several researchers (Abuel-Naga et al. 2007; Del Olmo et al. 1996). Results are included in Table 3 and the correlation between ε^{Tp} and overconsolidation ratio (OCR) is displayed in Fig. 10. Results of ε^{Tp} are based on samples with different clay mineralogy and measured under different temperature cycles, so a normalized value $\varepsilon^{Tp}/\varepsilon_{OCR=1}^{Tp}$ was used in Fig. 10. Generally, thermal plastic strain decreases nonlinearly with the overconsolidation ratio (OCR). At normally consolidated conditions (OCR = 1), the sample has the maximum amount of irreversible contraction upon heating; at overly consolidated condition (OCR > 3), small irreversible contraction or even dilation (expansion) can be generated in the sample. As shown in Fig. 10, an empirical coefficient F_o as a function of OCR was proposed to take into account the effect of stress history or OCR on the thermal plastic strain behavior. Under heating, anisotropic expansion of clay platelets and interlayer bound water will

result in local shear stress. When the thermally induced shear stress reaches the yielding limit of soft mudrocks, thermal plastic strains will be created. The mechanism of contraction or expansion in thermal plastic strains can be interpreted by the modified Cam-Clay plastic model (Wood 1991) as shown in Fig. 11. When a sample is heated at a stress state with low OCR (close to 1), plastic yielding will induce contraction. If the sample is heated at a stress state with an OCR around 3.5, small or no plastic strain is generated. If the sample is at a stress state with very high OCR (>>3), plastic yielding can induce some amount of dilation or expansion.

Finally, the component of thermal plastic strain will be expressed by:

$$d\varepsilon^{Tp} = -c_m f_{cw} F_o \frac{\Delta e_{cw}^{Tp}}{1+e_{cw0}} \tag{28}$$

Due to the oriented fabric in soft mudrocks, plastic strain (grain rearrangement) tends to happen along the normal direction of the fabric. Assuming that thermal plastic strain has the similar anisotropic behavior as the strain caused by clay dehydration, the thermal plastic strains along the x- and z- directions, $d\varepsilon_x^{Tp}$ and $d\varepsilon_z^{Tp}$ are derived as:

$$\begin{cases} d\varepsilon_x^{Tp} = 8\int_0^{\frac{\pi}{2}}\int_0^{\theta^f} d\varepsilon^{Tp} f(\theta^f)\sin\gamma\cos\beta\sin\gamma d\gamma d\beta \\ d\varepsilon_z^{Tp} = 8\int_0^{\frac{\pi}{2}}\int_0^{\theta^f} d\varepsilon^{Tp} f(\theta^f)\cos\gamma\sin\gamma d\gamma d\beta \end{cases} \tag{29}$$

4. Model validation

A series of thermal tests were conducted on reconstituted and natural soft mudrock samples with different clay fractions to validate the proposed compositional thermal strain model. Two reconstituted mudrock samples (brine saturated smectite-quartz mixtures) were prepared in the laboratory. A slurry of brine-saturated smectite-quartz mixtures was poured into an oedometer cell and consolidated up to a vertical effective stress of 10 MPa in a week. Two samples with

clay fractions of 0.2 and 0.45 marked as SQ1 and SQ2, respectively, were prepared according to the above-mentioned procedures. The reconstituted mudrock samples have the similar swelling characteristic with that of natural soft mudrock samples (Li and Wong 2016). Natural soft mudrock samples were retrieved from two heavy oil fields in the Western Canadian Sedimentary Basin (WCSB). The clay mineral is mainly made up of an illite-smectite (I-S) mixture, and smectite is dominant in the mixture. Non-clay minerals are mainly composed of quartz and a small amount of heavy mineral such as pyrite. Tests include high temperature oedometer tests, high temperature triaxial test with X-ray Computed Tomography (CT) scanning, and high temperature triaxial tests with local strain measurements. Details of the experiments and sample descriptions can be found at Li (2015). Some published thermal deformation data on the Boom clay was also used. Table 3 summarizes the test type, test conditions, sample description and some physical properties. Clay mineralogy and composition data for natural mudrock samples are based on XRD analysis results. All the samples contain a considerable amount of smectite. Porosity results are derived from bulk density data. The fabric angle results are estimated based on values of e_{cw} and the empirical equation proposed by Li and Wong (2017). Stress histories of reconstituted smectite-quartz samples and Boom clay samples are available and exact values of OCR are determined. The OCRs of WCSB shallowly buried shale samples are based on the preconsolidation stress measurement from Mohamadi and Wan (2015) and descriptions of the geological stress history by Gillott (1986). As shown in Fig. 12, the structural state values (c_m) of those samples range from the framework-supported state to the clay matrix-supported state.

4.1 High temperature oedometer tests

High temperature oedometer tests were performed on two reconstituted mudrock samples (brine saturated smectite-quartz mixtures) SQ1 and SQ2 to investigate their thermally induced

deformation behaviors (Table 3). At an OCR of 3.3, both samples displayed significant thermal expansion behavior. At the same temperature, the sample with a higher clay fraction (SQ2) displays a thermal expansion larger than the sample with a lower clay fraction (SQ1). The 1D thermal expansion behavior was modeled by applying the proposed compositional thermal strain model and displayed in Fig. 13. Measured and modeled points at the temperature of 73°C are comparable, but display significant differences for points at the temperature of 45°C. The discrepancy could result from calibration error during measurement.

4.2 High temperature triaxial test with X-ray CT scanning

Measured thermal strain behavior of the sample WCSB1 was displayed in Fig. 14. A trend of nonlinear thermal expansion behavior was observed. The slope starts to change when the temperature is higher than 53°C. Thermal plastic strain does not contribute to the thermal contraction behavior since the sample has an OCR of 3.5. The clay dehydration could be the reason of having nonlinear thermal strain behavior. There might be some overestimate in the measured thermal strains because the applied GE9800 CT scanner only has a resolution of 0.195 mm in a pixel. The trend of nonlinear thermal expansion behavior was modeled by using the proposed thermal strain model. However, the measured and modeled thermal expansion behavior have a significant difference in the magnitude. It is expected that the discrepancy will be reduced if a higher resolution CT scanner was used in the test.

4.3 High temperature triaxial tests with local strain measurements

Measured anisotropic thermal strains of samples WCSB2 and WCSB3 are shown in Fig. 15. Similarly, those samples have OCRs about 3.5, the thermal plastic deformation will contribute a limited amount of total thermal strain. The sample with a higher clay fraction (WCSB2) displays significant nonlinear and anisotropic thermal expansion behaviors, where the expansion along

the axial-direction (z-direction) is larger than that along the radial-direction (x-direction) of the sample. In contrast, the sample with a lower clay fraction (WCSB3) tends to have a very little difference in the thermal expansion behavior. The significant nonlinear and anisotropic thermal strain behavior of sample WCSB2 could be due to a large amount of clay-bound water in the sample. The slope change at the temperature about 60°C corresponds to the beginning of clay dehydration. The anisotropic thermal strain behaviors have been modeled using the proposed compositional thermal strain model.

Similar to the above-mentioned high temperature triaxial setup, series of drained heating and cooling tests at different constant effective isotropic stress values were performed by Del Olmo et al. (1996) to quantify thermal strain of Boom clay samples. The strain was calculated from the volume of water expelled from the specimen during heating. The sample (BoomClay1) has a high clay fraction and a high c_m value (Fig. 12). Other information on the Boom clay sample and testing conditions can be found in Table 3. Measured thermal strains at different OCRs for sample Boom Clay1 are displayed in Fig. 16. The sample displays significant thermal contraction behavior at low OCR and thermal expansion behavior at high OCR. Not like the contraction due to clay dehydration which initiates at a temperature higher than 50°C, thermal plastic deformation starts from the start of heating. During the process of cooling, the component of thermal plastic strain does not recover. Curves have flat sections when the sample was cooled from a temperature of 95°C to 50°C under different OCRs. This behavior corresponds to a process of clay rehydration which compensates the changes in dimensions of solid minerals and interlayer bound water due to cooling. As shown in Fig. 16, the thermal strain behaviors have been modeled using the compositional thermal strain model.

5. Discussions

5.1 Specific surface area

Specific surface captures the combined effects of particle size and slenderness in a measurement that is independent and complementary to grain-size distribution of fine-grained geomaterials (Santamarina et al. 2002). The total specific surface area covers all the pore space of a mudrock, but the external specific surface area does not cover the interlayer pore space of clay mineral (smectite). Theoretically, the specific surface area of soft mudrock has a linear correlation with the clay fraction as:

$$S_m = \frac{S_{nc}m_{nc} + S_c m_c}{m_{nc} + m_c} = S_{nc} + c_f (S_c - S_{nc}) \tag{30}$$

where S_m is the specific surface area based on solid mass for mudrock, S_{nc} and S_c are specific surface areas based on solid mass for non-clay minerals and clay minerals, respectively. The external specific surface area, S_{nc}^e and total specific surface area, S_{nc}^t for non-clay minerals are the same since there is no interlayer pore space. The external specific surface area, S_{inc}^e and total specific surface area, S_{inc}^t for non-clay minerals are the same. Sizes of non-clay minerals in mudrock range from 2 μm to 80 μm (Dewhurst et al. 1999; Gautam 2004; Schneider 2011). The value of Brunauer, Emmett and Teller (BET) specific surface area of silt at such size range is about 3 m^2/g (Parry et al. 2011). The same value will be used for the specific surface area of non-clay minerals, S_{nc}^e. Values of specific surface area for clay minerals depend on measurement methods and clay mineralogy. In the well-known nitrogen gas-adsorption technique, the BET approach measures external specific surface area, S_c^e for clay minerals (Santamarina et al. 2002). External specific surface area, S_m^e values for some smectite rich soft mudrocks or stiff clay from

different sites were plotted against the clay fractions and shown in Fig. 17. Samples include London Clay mudstone (Dewhurst et al. 1999), Norwegian margin mudstone (Yang and Aplin 1998), Nankai mudstone (Schneider 2011), Boom clay (Al-Mukhtar et al. 1996), and some natural shales (Kuila and Prasad 2013). Details on the sample descriptions can be found at Li (2015). In general, London Clay mudstones have higher specific surface area values than mudrocks from other sites. A major trend can be modeled based on Eq. (31) by applying the approach of linear regression and displayed in Fig. 17.

$$S_m^e = 3 + c_f (S_c^e - 3) \tag{31}$$

An estimated value of S_c^e for smectite-rich soft mudrocks is determined as 60 m^2/g.

5.2 Relevance to phenomenon-based thermal elastic-plastic model

Phenomenon-based thermal elastoplastic models have been proposed to simulate the thermal-mechanical behavior of clay-related geomaterials (Laloui and Cekerevac 2008; Sultan et al. 2002). Thermal elastoplastic parameters of those models should be obtained based on thermal mechanical tests. Laboratory tests can only provide a limited amount of characterization results on some samples, and thermal elastic-plastic properties of samples with different clay fractions still have large uncertainties. The clay mineral types may not have huge variations studying in a geological formation. However, soft mudrock samples retrieved from the same formation could have significant variations with burial depths (Day-Stirrat et al. 2012; Li and Wong 2016). The proposed compositional strain model investigates the effect of clay fraction on the deformation behavior in a quantitative way. The nonlinear thermal deformation behavior of soft mudrocks with different clay fractions can be estimated using the composition thermal strain model based on clay mineralogy, composition, and porosity data. Parameters in phenomenon-based thermal elastic-plastic models can be derived according to the estimated thermal strain curves. It should

be noted that the proposed correlation between void ratio change in clay-water composites (induced by thermal plastic strain), Δe_{cw}^{Tp} and temperature in this study is based on experimental results on Boom clay which is rich in the smectite mineral (Fig. 9). For a studied area with different clay mineralogy, it is recommended to perform a test on a sample with the highest clay fraction and develop the correlation between Δe_{cw}^{Tp} and temperature. Effect of clay fraction on mechanical parameters at the room temperature (e.g., compression index and friction angle) is included in Li and Wong (2016).

The proposed compositional thermal strain model has not taken into account mineral transformations in soft mudrocks. If some mineral transformation occurs during clay dehydration, (e.g., smectite to illite transformation), the contraction behavior due to clay dehydration will not be reversible and a higher amount of thermal plastic strain is expected (Hueckel and Pellegrini 2002). It is not clear that how thermal plastic strains develop in soft mudrocks under very high temperature condition (e.g., T >250°C). Further experiments are required to investigate the thermal plastic behavior due to mineral transformations.

5.3 Effect of dehydration from interlayer pore space

In some engineering activities such as thermal recovery and nuclear waste disposal, very long periods of heating operations on high clay fraction soft mudrocks are involved. It is necessary to look into the thermal deformation behavior when all clay-bound water is able to be depleted due to a long period of heating. Considering sample WCSB1 as an example, the total specific surface of bulk clay minerals is determined as 320 m^2/g based on the information of f_{sc} and total specific surface clay minerals, which are reported by Santamarina et al. (2002) as 500 m^2/g and 50 m^2/g for smectite and other clay minerals, respectively. Based on the proposed compositional thermal strain model, anisotropic thermal contraction behavior of the sample is estimated and shown in

Fig. 18. Very significant thermal contraction along the vertical- (z-) direction would be expected. During thermal recovery (e.g., cyclic steam stimulation), a large amount of deviated wells are used to conduct steam injection or oil production. Significant thermal contraction along the vertical direction of soft mudrocks may cause some wellbore integrity problem because the wellbore tends to lose the confinement after the long period of heating.

6. Conclusions

A compositional thermal strain model was proposed to investigate the anisotropic thermal strain behavior of soft mudrocks by examining the mineral composition and micro-scale structure. The proposed model was validated by measured results on reconstituted and natural soft mudrocks or dense clays. The proposed thermal strain model can be applied to estimate the thermal deformation parameters in phenomenon-based thermal elastic-plastic models. Several conclusions were drawn as follows:

- The mechanisms of thermal strain in soft mudrocks are due to the expansion of solid minerals and interlayer bound water, the removal or dehydration of clay-bound water, and thermal plastic strain (grain rearrangement). Water saturated soft mudrocks can be treated as a mixture composed of non-clay minerals and clay-water composites. The overall deformation of soft murocks is contributed by the thermal deformation behavior of individual constituents and their interactions. The interactions among non-clay minerals and clay-water composites can be considered by using the structural state model.
- Thermally induced clay dehydration can be quantified based on clay mineralogy composition and porosity data. Strain due to clay dehydration could lead to nonlinear thermal strain behavior in high clay fraction samples even if there are no thermal plastic

strains. A full clay dehydration process including the removal of all clay-bound water in the interlayer pore space of a soft mudrock may lead to considerable thermal contraction behavior in a high OCR sample but it requires a long period of time.

- The anisotropy in thermal strain behavior of soft mudrocks can be quantified based on the anisotropy in the oriented fabric. Anisotropic thermal expansion behavior of interlayer clay-bound water and solid clay minerals are major sources of anisotropic thermal expansion strains. Clay dehydration and anisotropic in particle rearrangement are major sources of anisotropic thermal contraction strains.

Acknowledgement

The authors would like to acknowledge the supports by BitCan Geosciences & Engineering Inc., Mitacs Canada, Imperial Oil Limited Canada, Concordia University ENCS start-up fund, and NSERC. The first author has been benefiting from the University of Calgary Eyes High International Doctoral Scholarship. Comments from two anonymous reviewers are beneficial for this paper.

References

Abuel-Naga, H.M., Bergado, D.T., and Bouazza, A. 2007. Thermally induced volume change and excess pore water pressure of soft Bangkok clay. Engineering Geology 89(1): 144-154. doi: http://dx.doi.org/10.1016/j.enggeo.2006.10.002.

Al-Mukhtar, M., Belanteur, N., Tessier, D., and Vanapalli, S.K. 1996. The fabric of a clay soil under controlled mechanical and hydraulic stress states. Applied Clay Science 11(2–4): 99-115. doi: http://dx.doi.org/10.1016/S0169-1317(96)00023-3.

Barry-Macaulay, D., Bouazza, A., Singh, R.M., Wang, B., and Ranjith, P.G. 2013. Thermal conductivity of soils and rocks from the Melbourne (Australia) region. Engineering Geology 164: 131-138. doi: http://dx.doi.org/10.1016/j.enggeo.2013.06.014.

Campanella, R.G., and Mitchell, J.K. 1968. Influence of temperature variations on soil behavior. Journal of the Soil Mechanics and Foundations Division 94(SM 3): 709-734.

Cariou, S., Dormieux, L., and Skoczylas, F. 2013. An original constitutive law for Callovo-Oxfordian argillite, a two-scale double-porosity material. Applied Clay Science 80–81(0): 18-30. doi: http://dx.doi.org/10.1016/j.clay.2013.05.003.

Cholach, P.Y., and Schmitt, D.R. 2006. Intrinsic elasticity of a textured transversely isotropic muscovite aggregate: Comparisons to the seismic anisotropy of schists and shales. Journal of Geophysical Research: Solid Earth 111(B9): B09410. doi: 10.1029/2005jb004158.

Colten-Bradley, V.A. 1987. Role of pressure in smectite dehydration; effects on geopressure and smectite-to-illite transformation. AAPG Bulletin 71(11): 1414-1427.

Day-Stirrat, R.J., Flemings, P.B., You, Y., Aplin, A.C., and van der Pluijm, B.A. 2012. The fabric of consolidation in Gulf of Mexico mudstones. Marine Geology 295: 77-85. doi: 10.1016/j.margeo.2011.12.003.

Day-Stirrat, R.J., Schleicher, A.M., Schneider, J., Flemings, P.B., Germaine, J.T., and van der Pluijm, B.A. 2011. Preferred orientation of phyllosilicates: Effects of composition and stress on resedimented mudstone microfabrics. Journal of Structural Geology 33(9): 1347-1358. doi: 10.1016/j.jsg.2011.06.007.

Del Olmo, C., Fioravante, V., Gera, F., Hueckel, T., Mayor, J.C., and Pellegrini, R. 1996. Thermomechanical properties of deep argillaceous formations. Engineering Geology 41(1–4): 87-102. doi: 10.1016/0013-7952(95)00048-8.

Demars, K.R., and Charles, R.D. 1982. Soil volume changes induced by temperature cycling. Canadian Geotechnical Journal 19(2): 188-194. doi: 10.1139/t82-021.

Derjaguin, B.V., Karasev, V.V., and Khromova, E.N. 1992. Thermal expansion of water in fine pores. Progress in Surface Science 40(1–4): 391-392. doi: http://dx.doi.org/10.1016/0079-6816(92)90067-R.

Dewhurst, D.N., Aplin, A.C., and Sarda, J.P. 1999. Influence of clay fraction on pore-scale properties and hydraulic conductivity of experimentally compacted mudstones. Journal of Geophysical Research-Solid Earth 104(B12): 29261-29274. doi: 10.1029/1999jb900276.

Di Donna, A., and Laloui, L. 2015. Response of soil subjected to thermal cyclic loading: Experimental and constitutive study. Engineering Geology 190: 65-76. doi: http://dx.doi.org/10.1016/j.enggeo.2015.03.003.

Folk, R.L. 1980. Petrology for sedimantary rocks. Hemphill Publishing Company, Austin, Texas.

Gautam, R. 2004. Anisotropy in deformations and hydraulic properties of Colorado shale. Ph.D. thesis, Department of Civil Engineering, University of Calgary, Calgary, Alberta.

Gillott, J.E. 1986. Some clay-related problems in engineering geology in North America. Clay Minerals 21(3): 261-278. doi: 10.1180/claymin.1986.021.3.02.

Gonçalvès, J., Rousseau-Gueutin, P., de Marsily, G., Cosenza, P., and Violette, S. 2010. What is the significance of pore pressure in a saturated shale layer? Water Resour. Res. 46(4): W04514. doi: 10.1029/2009wr008090.

Hueckel, T., and Baldi, G. 1990. Thermoplasticity of saturated clays: experimental constitutive study. Journal of Geotechnical Engineering 116(12): 1778-1796. doi: doi:10.1061/(ASCE)0733-9410(1990)116:12(1778).

Hueckel, T., and Pellegrini, R. 1996. A note on thermomechanical anisotropy of clays. Engineering Geology 41(1): 171-180. doi: http://dx.doi.org/10.1016/0013-7952(95)00050-X.

Hueckel, T., and Pellegrini, R. 2002. Reactive plasticity for clays: application to a natural analog of long-term geomechanical effects of nuclear waste disposal. Engineering Geology 64(2): 195-215. doi: http://dx.doi.org/10.1016/S0013-7952(01)00114-4.

Hüpers, A., and Kopf, A.J. 2009. The thermal influence on the consolidation state of underthrust sediments from the Nankai margin and its implications for excess pore pressure. Earth and Planetary Science Letters 286(1–2): 324-332. doi: http://dx.doi.org/10.1016/j.epsl.2009.05.047.

Ichikawa, Y., and Selvadurai, A.P.S. 2012. Transport phenomena in porous media aspects of micro/macro behaviour. Springer, Berlin; New York.

Jia, Y., Bian, H.B., Duveau, G., Su, K., and Shao, J.F. 2009. Numerical modelling of in situ behaviour of the Callovo–Oxfordian argillite subjected to the thermal loading. Engineering Geology 109(3): 262-272. doi: http://dx.doi.org/10.1016/j.enggeo.2009.08.012.

Kuila, U., and Prasad, M. 2013. Specific surface area and pore-size distribution in clays and shales. Geophysical Prospecting 61(2): 341-362. doi: 10.1111/1365-2478.12028.

Laloui, L., and Cekerevac, C. 2008. Numerical simulation of the non-isothermal mechanical behaviour of soils. Computers and Geotechnics 35(5): 729-745. doi: http://dx.doi.org/10.1016/j.compgeo.2007.11.007.

Li, B. 2015. Effect of clay fraction on thermal-hydro-mechanical responses of soft mudrocks. Ph.D. thesis, Department of Civil Engineering, University of Calgary, Calgary, Alberta.

Li, B., and Wong, R. 2015. Effect of heating in steam-based-oil-recovery process on deformation of shale: a compositional thermal strain model. Journal of Canadian Petroleum Technology 54(1): 26-35.

Li, B., and Wong, R.C.K. 2016. Quantifying structural states of soft mudrocks. Journal of Geophysical Research: Solid Earth 121(5): 3324-3347. doi: 10.1002/2015JB012454.

Li, B., and Wong, R.C.K. 2017. Modeling anisotropic static elastic properties of soft mudrocks with different clay fractions. Geophysics 82(1): MR27-MR37. doi: 10.1190/geo2015-0575.1.

Ma, Y.-S., Chen, W.-Z., Yu, H.-D., Gong, Z., and Li, X.-L. 2016. Variation of the hydraulic conductivity of Boom Clay under various thermal-hydro-mechanical conditions. Engineering Geology 212: 35-43. doi: http://dx.doi.org/10.1016/j.enggeo.2016.07.013.

McKinstr, H.A. 1965. Thermal expansion of clay minerals. American Mineralogist 50(1-2): 212-222.

Mitchell, J.K., and Soga, K. 2005. Fundamentals of soil behavior, 3rd Edition. J. Wiley & Sons, New York.

Mohamadi, M., and Wan, R.G. 2015. Influence of structuration on the critical state friction angle: an elastoplastic description. In The 49th US Rock Mechanics/Geomechanics Symposium. American Rock Mechanics Association, San Francisco, CA, USA.

Moyano, B., Spikes, K.T., Johansen, T.A., and Mondol, N.H. 2012. Modeling compaction effects on the elastic properties of clay-water composites. Geophysics 77(5): D171-D183. doi: 10.1190/geo2011-0426.1.

Munson, B.R., Young, D.F., and Okiishi, T.H. 2002. Fundamentals of fluid mechanics. Wiley, New York.

Murray, H.H. 2007. Applied clay mineralogy: Occurrences, processing, and application of kaolins, bentonites, palygorskite-sepiolite, and common clays. Elsevier, Amsterdam; Boston.

Parry, S.A., Hodson, M.E., Oelkers, E.H., and Kemp, S.J. 2011. Is silt the most influential soil grain size fraction? Applied Geochemistry 26, Supplement(0): S119-S122. doi: http://dx.doi.org/10.1016/j.apgeochem.2011.03.045.

Robertson, E.C. 1988. Thermal properties of rocks. U.S. Dept. of the Interior, Geological Survey

Santamarina, J.C., Klein, K.A., Wang, Y.H., and Prencke, E. 2002. Specific surface: determination and relevance. Canadian Geotechnical Journal 39(1): 233-241. doi: 10.1139/t01-077.

Schneider, J. 2011. Compression and permeability behavior of natural mudstones. Ph.D. thesis, Department of Geological Sciences, The University of Texas at Austin, Austin, Texas.

Skinner, B.J. 1966. Thermal Expansion. In: Clark, JR. S.P. (ed.), Handbook of Physical Constants. Revised Edition. The Geological Society of America, Inc., Memoir 97. pp. 75-96

Sultan, N., Delage, P., and Cui, Y.J. 2002. Temperature effects on the volume change behaviour of Boom clay. Engineering Geology 64(2-3): 135-145. doi: 10.1016/s0013-7952(01)00143-0.

Vidal, O., and Dubacq, B. 2009. Thermodynamic modelling of clay dehydration, stability and compositional evolution with temperature, pressure and H2O activity. Geochimica Et Cosmochimica Acta 73(21): 6544-6564. doi: 10.1016/j.gca.2009.07.035.

Wong, R.C.K., Schmitt, D.R., Collis, D., and Gautam, R. 2008. Inherent transversely isotropic elastic parameters of over-consolidated shale measured by ultrasonic waves and their comparison with static and acoustic in situ log measurements. Journal of Geophysics and Engineering 5(1): 103-117. doi: 10.1088/1742-2132/5/1/011.

Wong, R.C.K., and Wang, E.Z. 1997. Three-dimensional anisotropic swelling model for clay shale - A fabric approach. International Journal of Rock Mechanics and Mining Sciences 34(2): 187-198. doi: 10.1016/s0148-9062(96)00057-5.

Wood, D.M. 1991. Soil Behaviour and Critical State Soil Mechanics. Cambridge University Press.

Yang, Y.L., and Aplin, A.C. 1998. Influence of lithology and compaction on the pore size distribution and modelled permeability of some mudstones from the Norwegian margin. Marine and Petroleum Geology 15(2): 163-175. doi: 10.1016/s0264-8172(98)00008-7.

Zhang, C.L., Wieczorek, K., and Xie, M.L. 2012. Swelling experiments on mudstones. Journal of rock mechanics and geotechnical engineering 2(1): 44-51. doi: 10.3724/SP.J.1235.2010.00044.

Zhao, Y.S., Wan, Z.J., Feng, Z.J., Xu, Z.H., and Liang, W.G. 2017. Evolution of mechanical properties of granite at high temperature and high pressure. Geomechanics and Geophysics for Geo-Energy and Geo-Resources 3(2): 199-210. doi: 10.1007/s40948-017-0052-8.

Table 1 **Measured anisotropic thermal expansion coefficients of some clay minerals (McKinstr, 1965).**

Mineral	α_1^c ($\times 10^{-6}$/°C)	α_2^c ($\times 10^{-6}$/°C)	Temperature range (°C)
Muscovite	17.8	3.5	25-600
Kaolinite	18.6	5.2	25-400
Chlorite	9.0	11.1	25-500

Table 2 Void ratio changes in fine-grained geomaterials induced by thermal plastic strain.

References	Description	Major clay minerals	c_f	ϕ	f_{cw}	T_1 (°C)	T_2 (°C)	ε^{Tp}	Δe^{Tp}	Δe_{cw}^{Tp}
Demars and Charles (1982)	Marine clay	Smectite	0.62	0.50	0.82	25	50	NA	0.025	0.039
Hueckel and Baldi (1990)	Pontida clay	Illite/Kaolinite	0.75	0.45	0.87	22	80	-0.013	NA	0.030
Del Olmo et al. (1996)	Boom clay	Smectite/Illite	0.62	0.29	0.74	22	95	-0.019	NA	0.037
Sultan et al. (2002)	Boom clay	Smectite/Illite	0.62	0.32	0.75	22	100	-0.033	NA	0.067
Sultan et al. (2002)	Boom clay	Smectite/Illite	0.62	0.37	0.77	20	70	NA	0.020	0.028
Abuel-Naga et al. (2007)	Bangkok clay	Smectite	0.69	0.62	0.89	25	90	-0.056	NA	0.212
Laloui and Cekerevac (2008)	Kaolinite	Kaolinite	0.69	0.41	0.82	22	90	-0.005	NA	0.012

Note: c_f = clay fraction; ϕ = porosity; f_{cw} = volume fraction of clay-water composites; T_1 and T_2 = temperatures at which the consolidation tests were conducted; ε^{Tp} = thermal plastic strain; Δe^{Tp} = void ratio change in bulk sample due to thermal plastic strain; Δe_{cw}^{Tp} = void ratio change in clay-water composites due to thermal plastic strain; NA = not available.

Table 3 Some properties of samples and testing conditions for thermal deformation measurements.

Experiments	Sample ID	Note	c_f	f_{sc}	ϕ	c_m	θ^f (°)	T range (°C)	σ' (MPa)	p_f (MPa)	OCR
Oedometer test	SQ1	Smectite-quartz mixtures	0.20	1	0.25	0.06	69.5	22-73	3	0	3.3
	SQ2	Smectite-quartz mixtures	0.45	1	0.26	0.39	38.5	22-73	3	0	3.3
X-ray CT scanning	WCSB1	Natural soft mudrock	0.48	0.6	0.29	0.5	22.5	20-129	2.8	3	3.5
Triaxial test	WCSB2	Natural soft mudrock	0.46	0.50	0.28	0.45	24.0	20-150	4.0	2.0	3.5
	WCSB3	Natural soft mudrock	0.22	0.25	0.25	0.07	51.1	20-78	2.4	1.0	3.5
	Boom Clay1	From Del Olmo et al. (1996)	0.62	0.54	0.35	0.81	33.2	22-95	1-6	0	1-6

f_{sc} = smectite fraction in clay minerals; c_m = coefficient of matrix, structural state value; θ^f = fabric angle; T = temperature; σ' = effective stress; p_f = pore fluid pressure; OCR = over consolidation ratio.

Figure Captions

Fig. 1 Sketches showing (a) soft mudrocks described as a four-scale material; (b) soft mudrocks with structural states of framework-supported and matrix-supported (Li and Wong 2016).

Fig. 2 Sketch illustrating thermally induced deformation behavior of clay-water composites.

Fig. 3 A solid clay mineral particle with preferred orientation in an overall coordinate system.

Fig. 4 Measured and modelled thermal strain behavior of bound water in nano-pore.

Fig. 5 Sketch illustrating two-scale flow behavior in a representative elementary volume (REV) of clay-water composites.

Fig. 6 Measured and modelled relationships between change of bound-water thickness, Δd and temperature.

Fig. 7 Sketch illustrating thermal effect on normal consolidation curve of fine-grained geomaterials (e = void ratio; σ' = effective stress). Modified after Li and Wong (2015).

Fig. 8 Measured void ratio changes in clay-water composites (induced by thermal plastic strain) at different temperatures.

Fig. 9 Measured and modelled relationship between void ratio change in clay-water composites (induced by thermal plastic strain) and temperature for soft mudrocks.

Fig. 10 Measured and modeled correlation between thermal plastic strain and overconsolidation ratio of fine-grained geomaterials.

Fig. 11 Sketch illustrating the mechanism of contraction or expansion in thermal plastic strains interpreted by the modified Cam-Clay plastic model (q = shear stress; p = mean effective stress; p_0 = pre-consolidation stress; CSL = critical state line; M = slope of critical state line).

Fig. 12 Structural states of samples for thermal deformation experiments.

Fig. 13 Measured and modeled 1D thermal deformation behavior of reconstituted smectite-quartz mixtures.

Fig. 14 Measured and modeled thermal volumetric strains of sample WCSB1 ($c_f = 0.48$).

Fig. 15 Measured and modeled anisotropic thermal strains of samples WCSB2 and WCSB3.

Fig. 16 Measured and modeled thermal volumetric strains of sample Boom Clay1.

Fig. 17. Measured and modeled relationship between external specific surface area and clay fraction.

Fig. 18 Estimated thermal contraction strain of sample WCSB1 due to the long term of thermally induced clay dehydration.

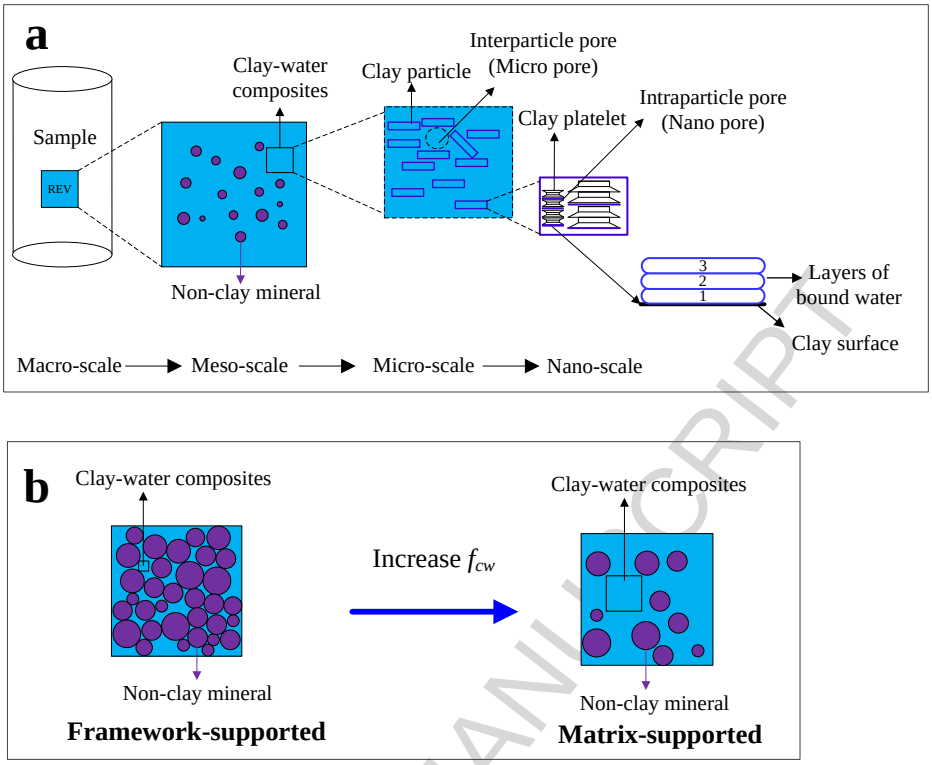

Fig. 1 Sketches showing (a) soft mudrocks described as a four-scale material; (b) soft mudrocks with structural states of framework-supported and matrix-supported (Li and Wong 2016).

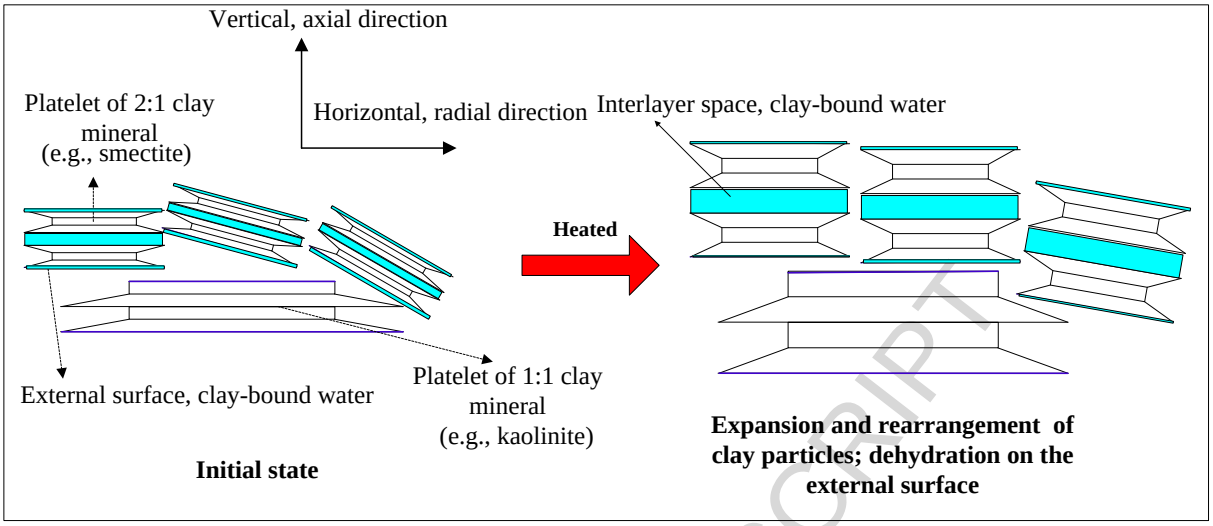

Fig. 2 Sketch illustrating thermally induced deformation behavior of clay-water composites.

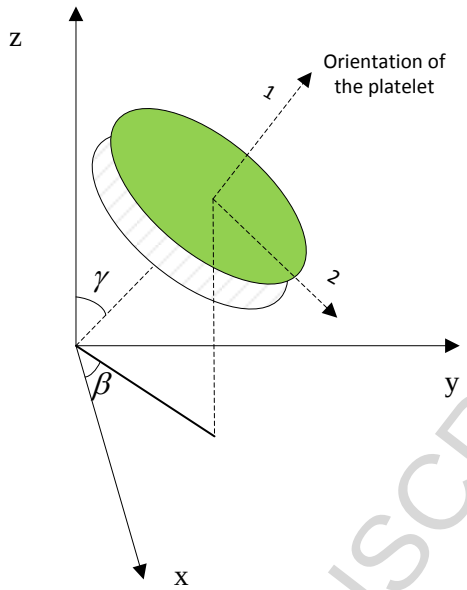

Fig. 3 A solid clay mineral particle with preferred orientation in an overall coordinate system.

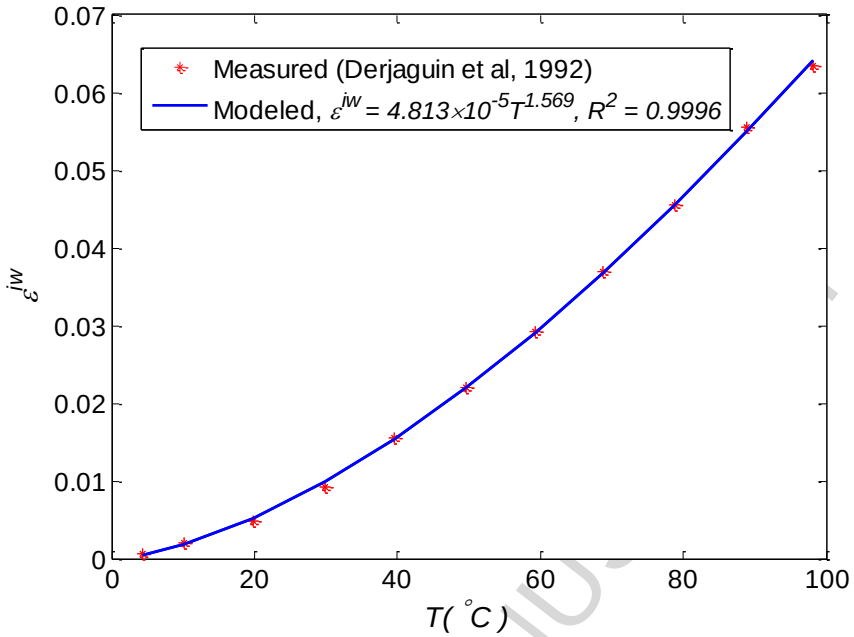

Fig. 4 Measured and modelled thermal strain behavior of bound water in nano-pore.

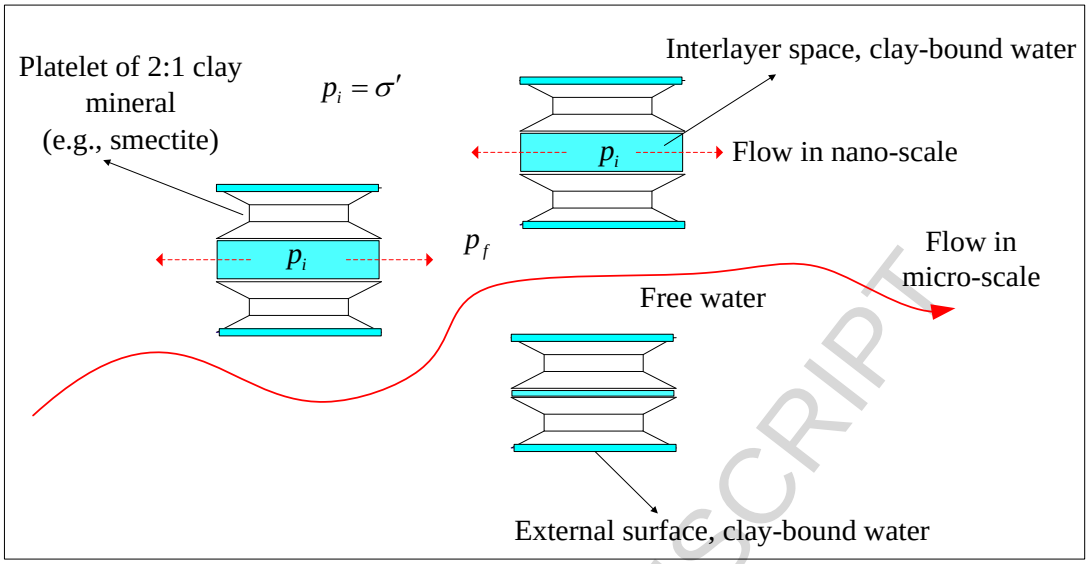

Fig. 5 Sketch illustrating two-scale flow behavior in a representative elementary volume (REV) of clay-water composites.

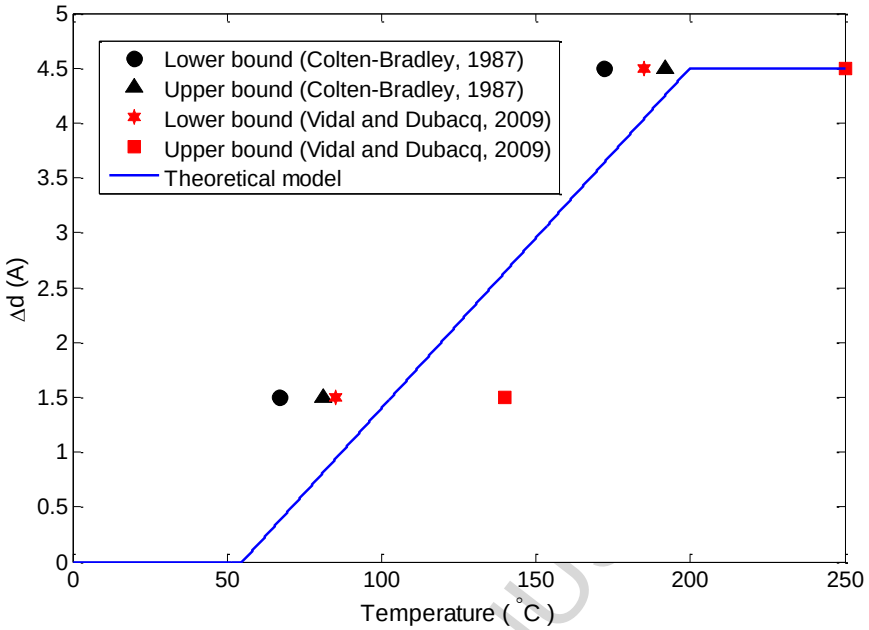

Fig. 6 Measured and modelled relationships between change of bound-water thickness, Δd and temperature.

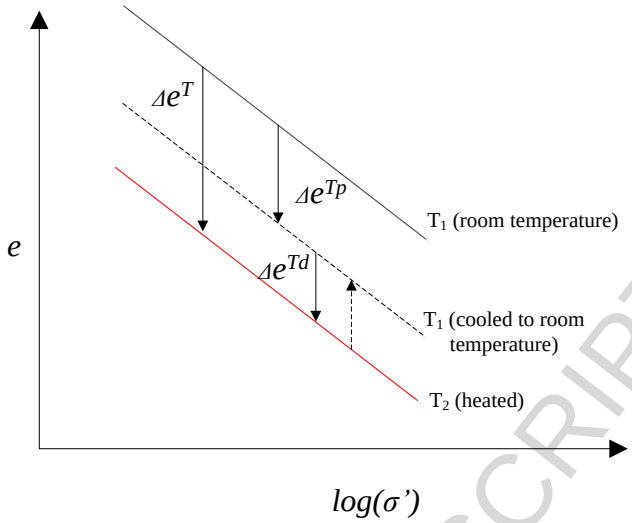

Fig. 7 Sketch illustrating thermal effect on normal consolidation curve of fine-grained geomaterials (e = void ratio; σ' = effective stress). Modified after Li and Wong (2015).

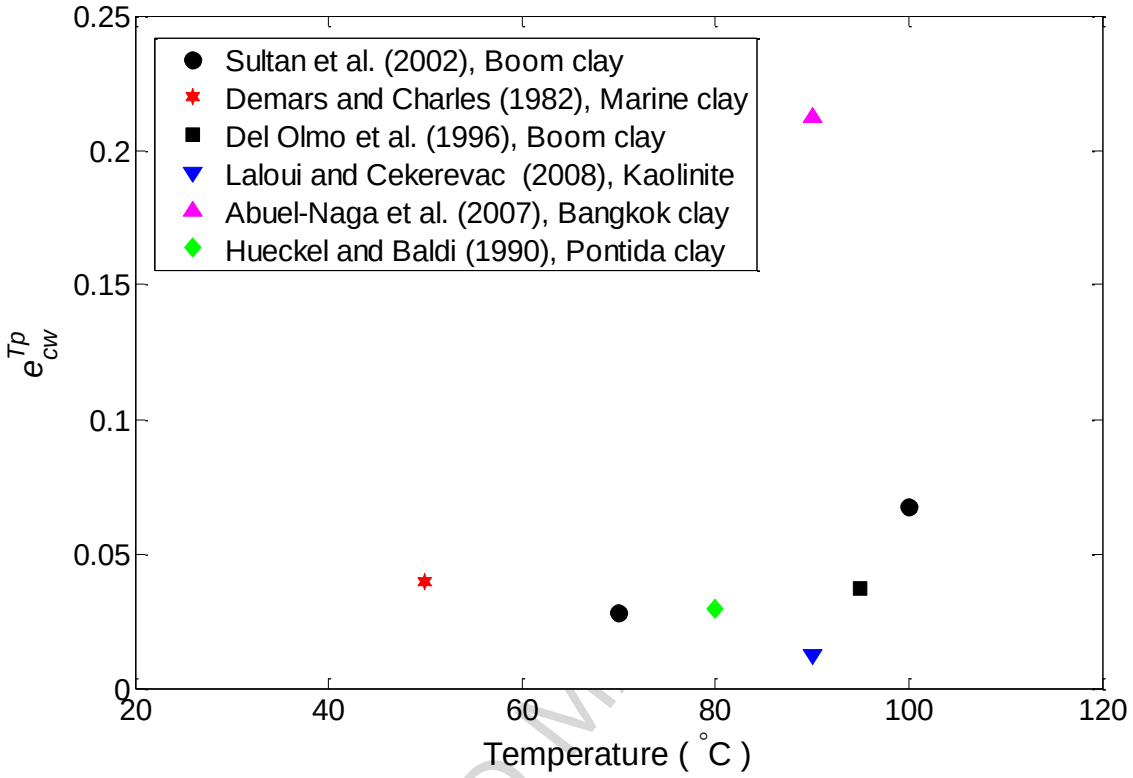

Fig. 8 Measured void ratio changes in clay-water composites (induced by thermal plastic strain) at different temperatures.

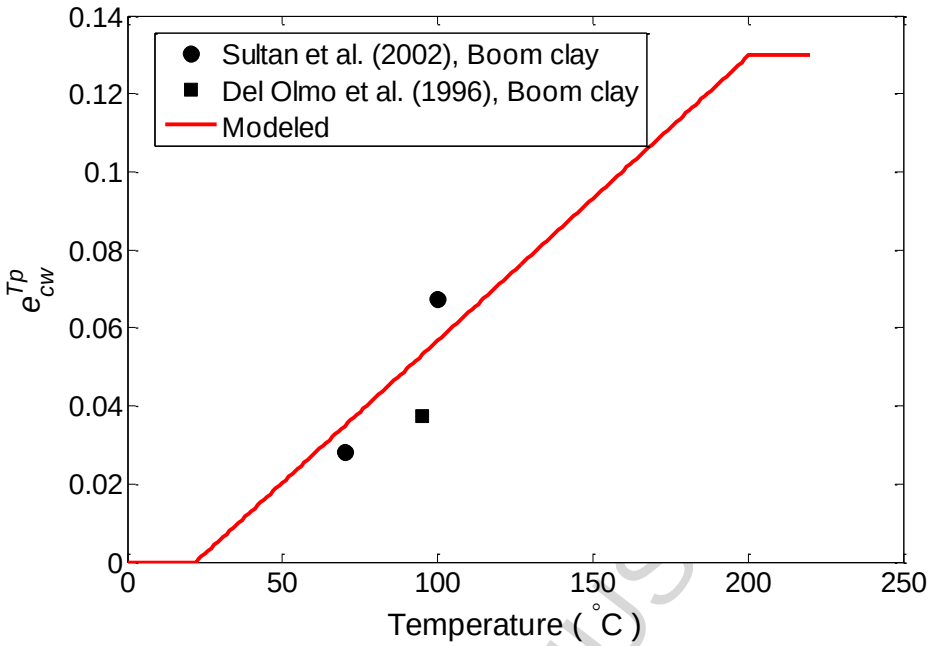

Fig. 9 Measured and modelled relationship between void ratio change in clay-water composites (induced by thermal plastic strain) and temperature for soft mudrocks.

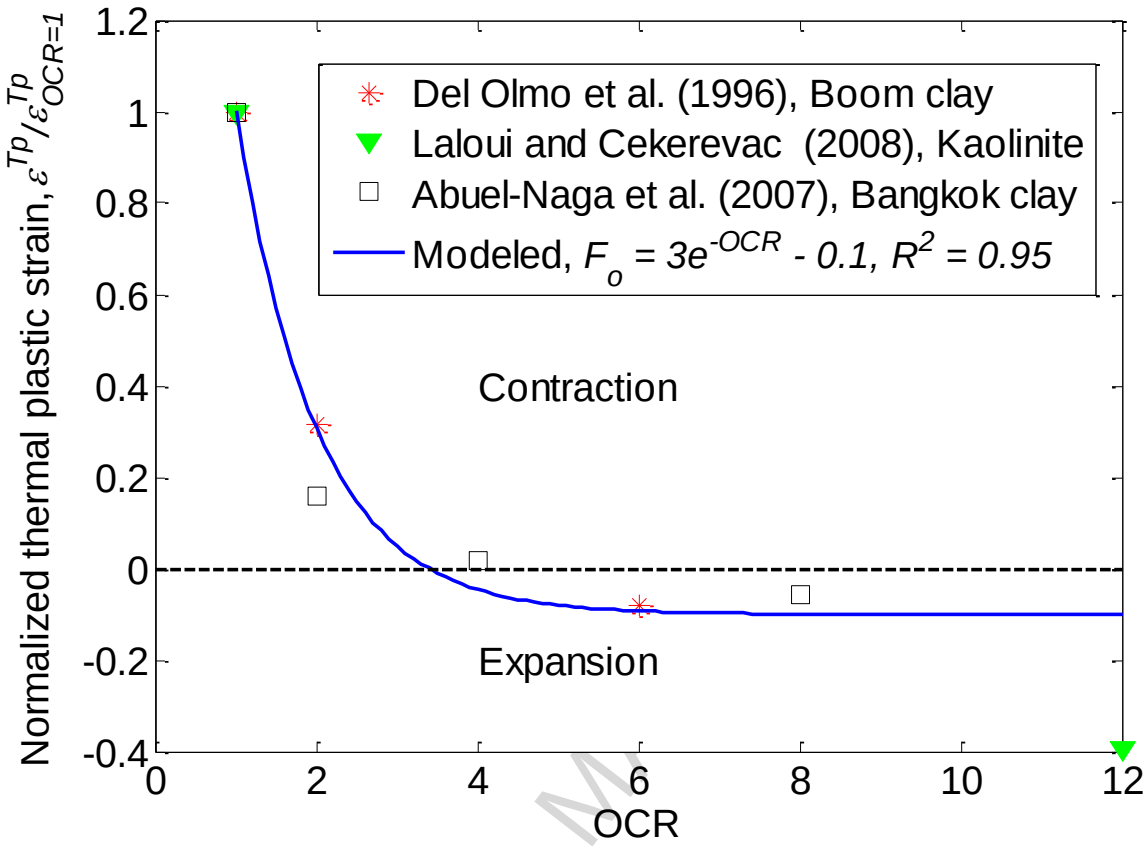

Fig. 10 Measured and modeled correlation between thermal plastic strain and overconsolidation ratio of fine-grained geomaterials.

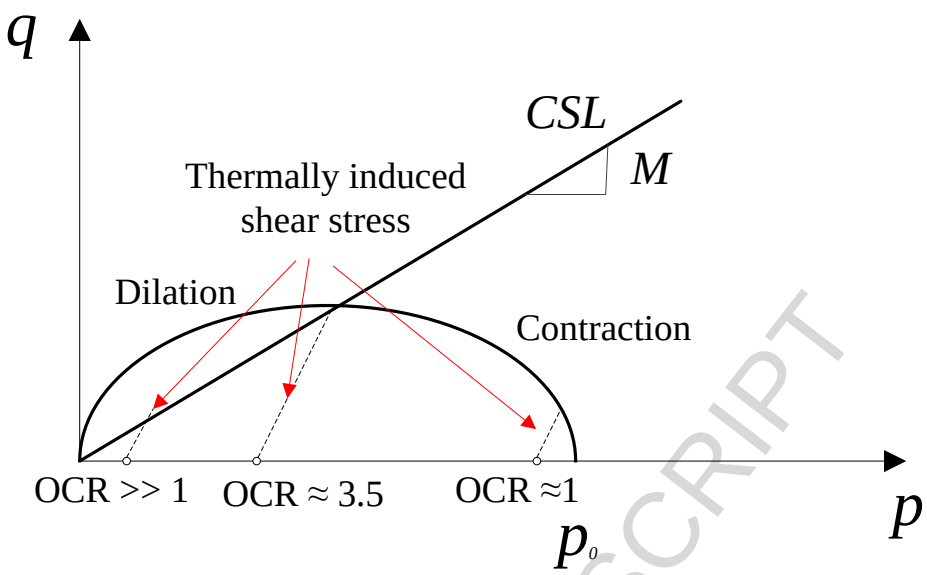

Fig. 11 Sketch illustrating the mechanism of contraction or expansion in thermal plastic strains interpreted by the modified Cam-Clay plastic model (q = shear stress; p = mean effective stress; p_0 = pre-consolidation stress; *CSL* = critical state line; M = slope of critical state line).

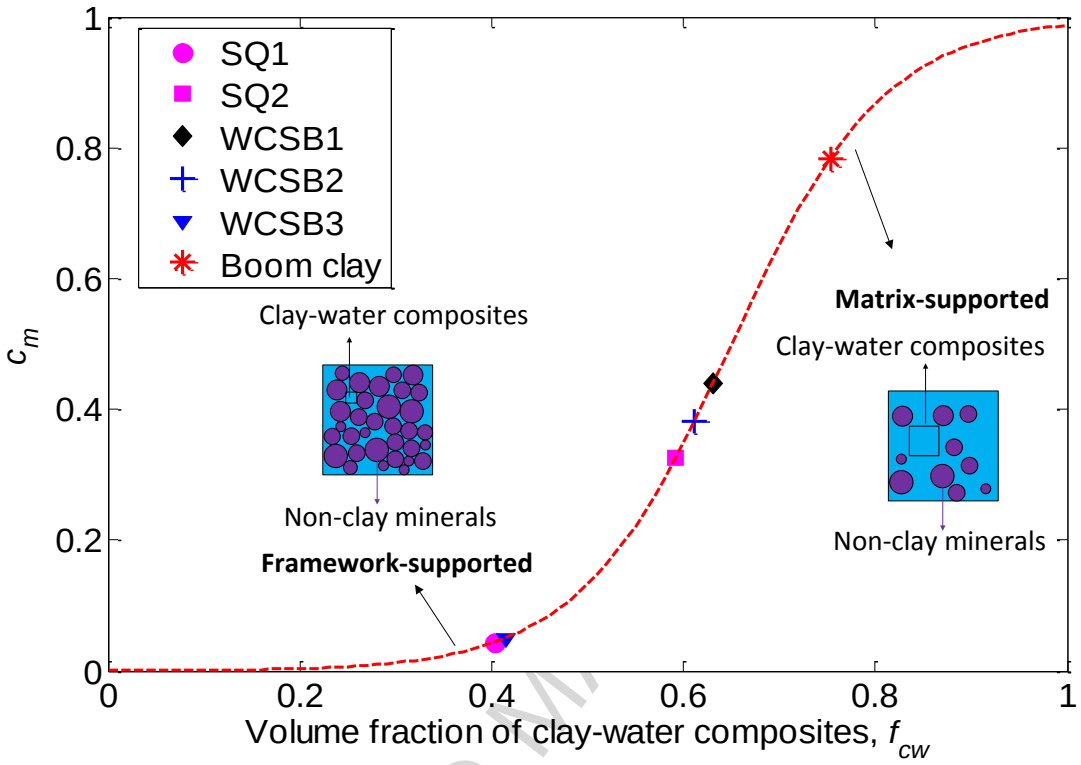

Fig. 12 Structural states of samples for thermal deformation experiments.

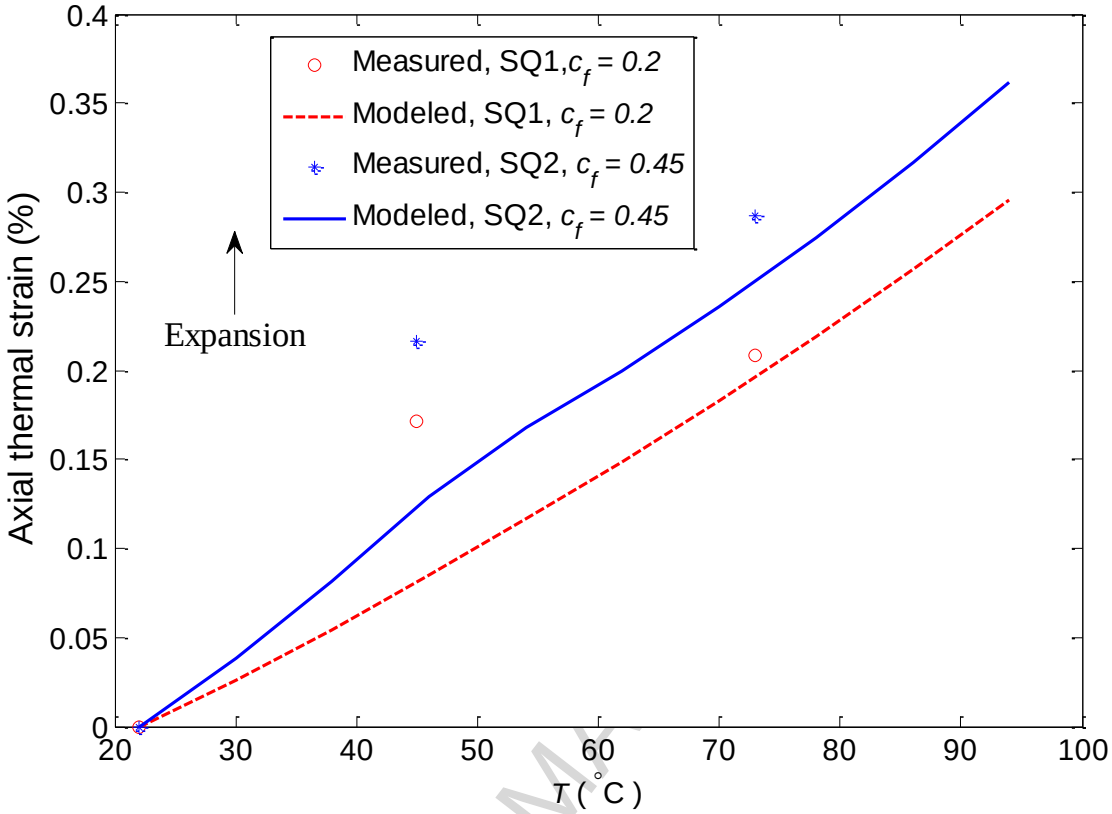

Fig. 13 Measured and modeled 1D thermal deformation behavior of reconstituted smectite-quartz mixtures.

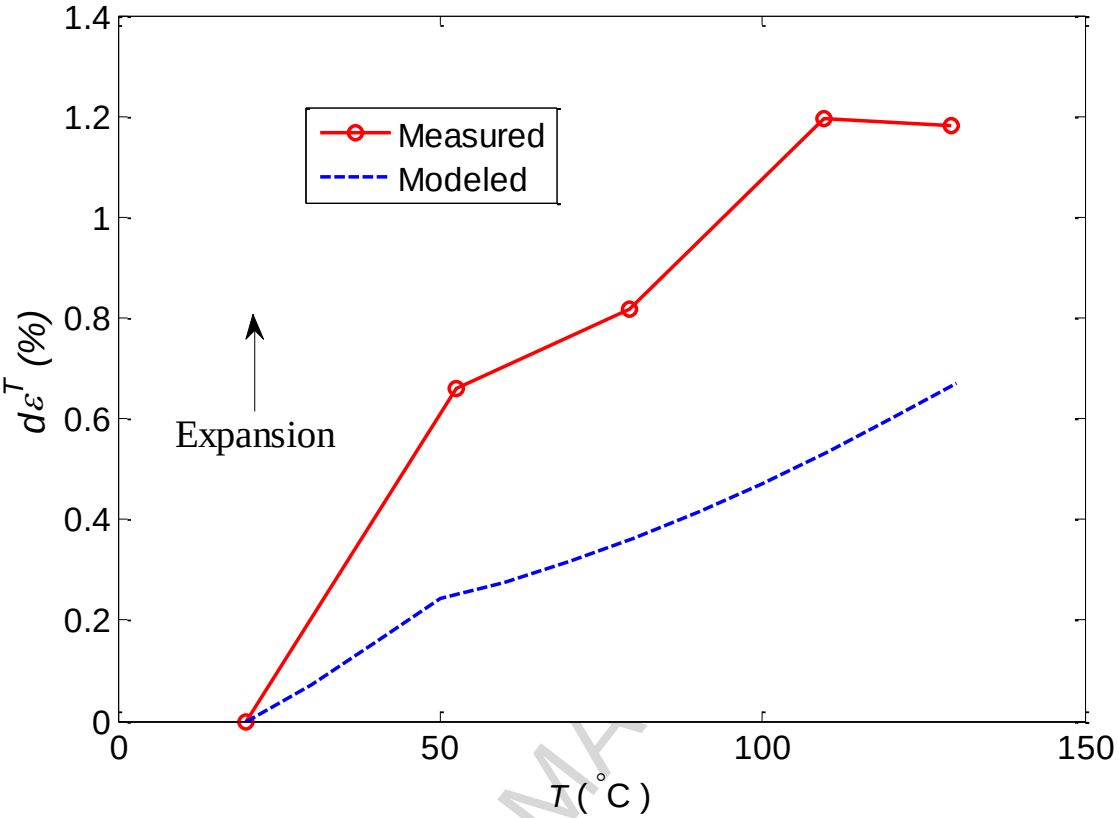

Fig. 14 Measured and modeled thermal volumetric strains of sample WCSB1 (c_f = 0.48).

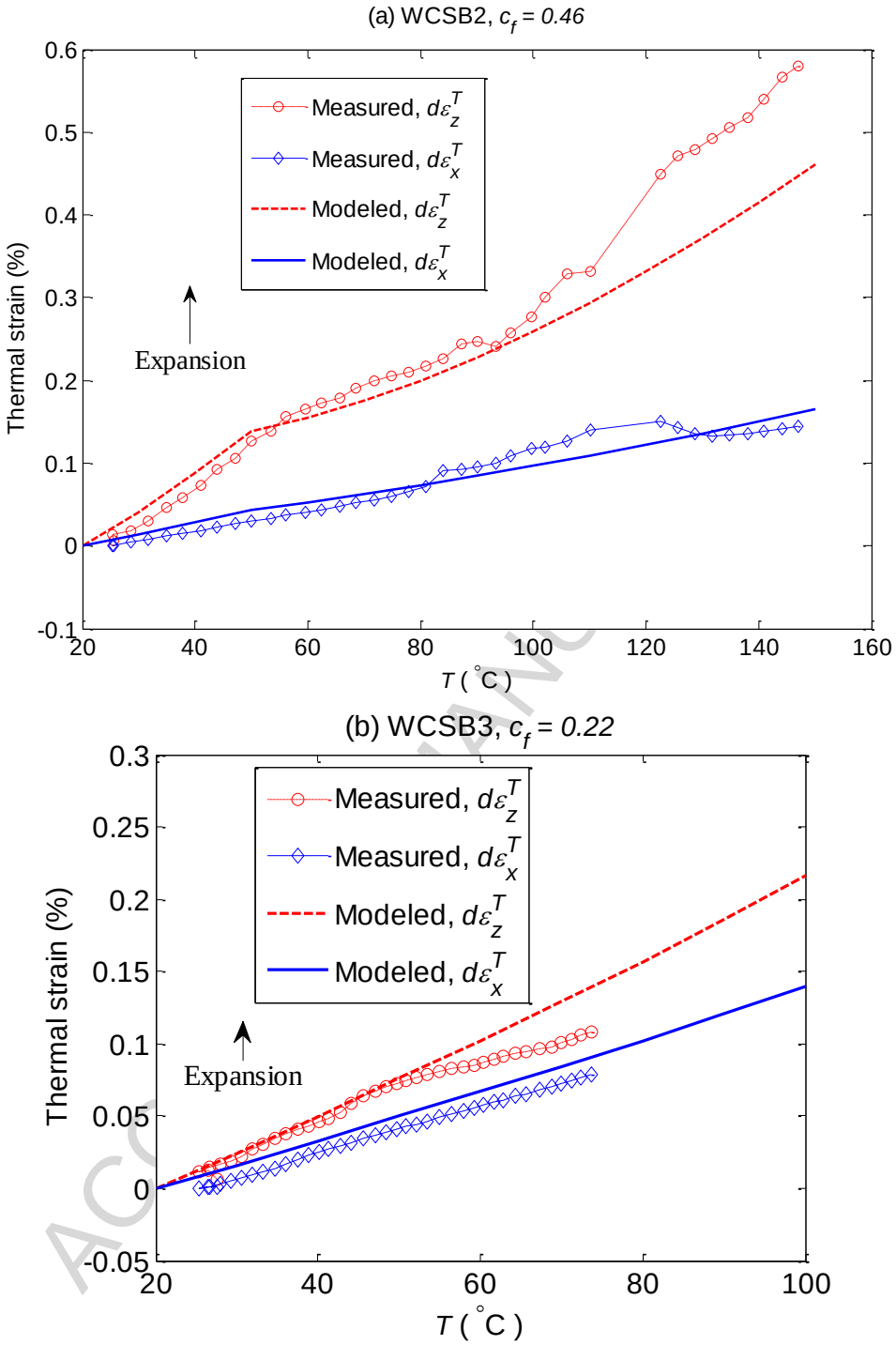

Fig. 15 Measured and modeled anisotropic thermal strains of samples WCSB2 and WCSB3.

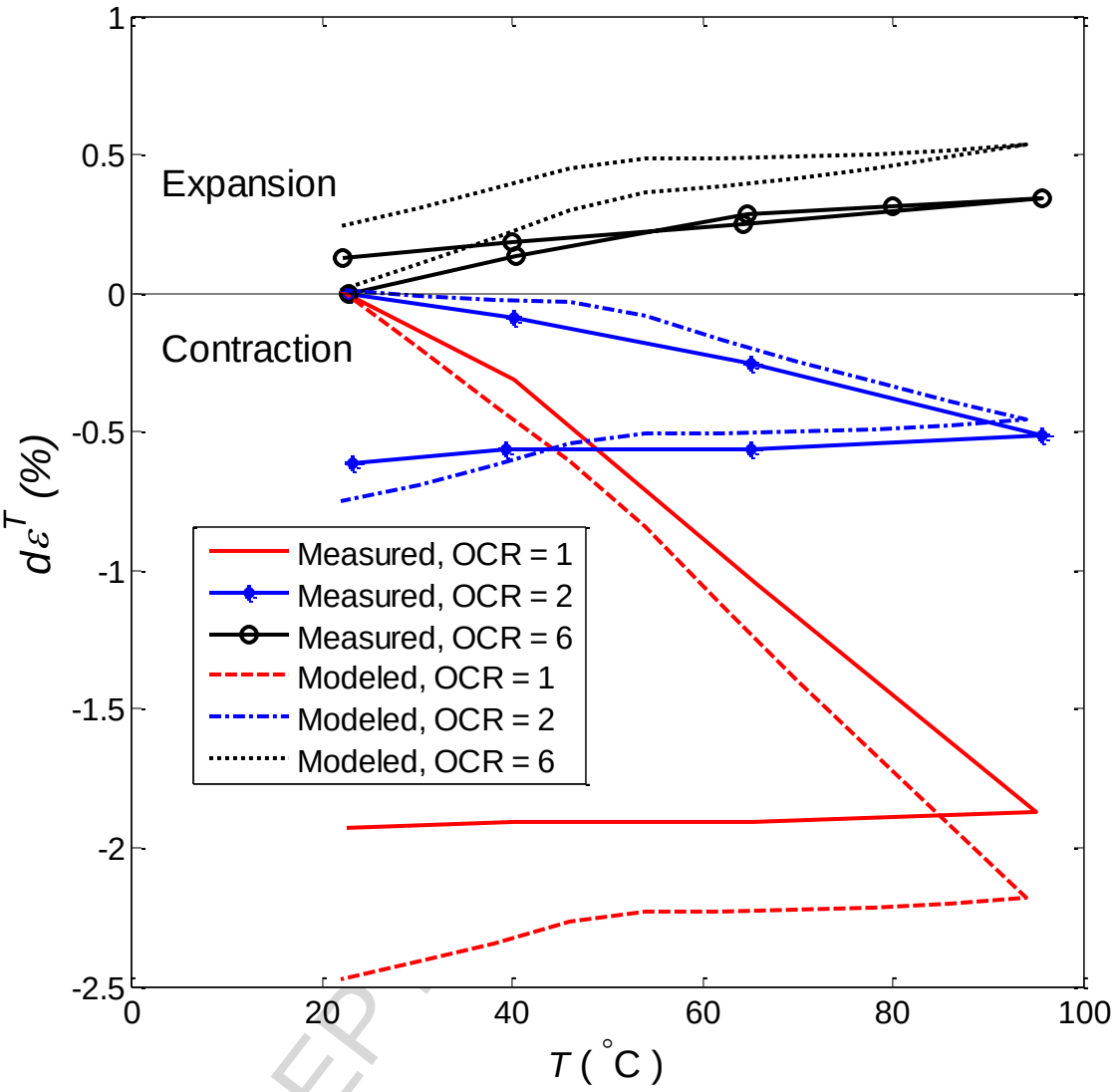

Fig. 16 Measured and modeled thermal volumetric strains of sample Boom Clay1.

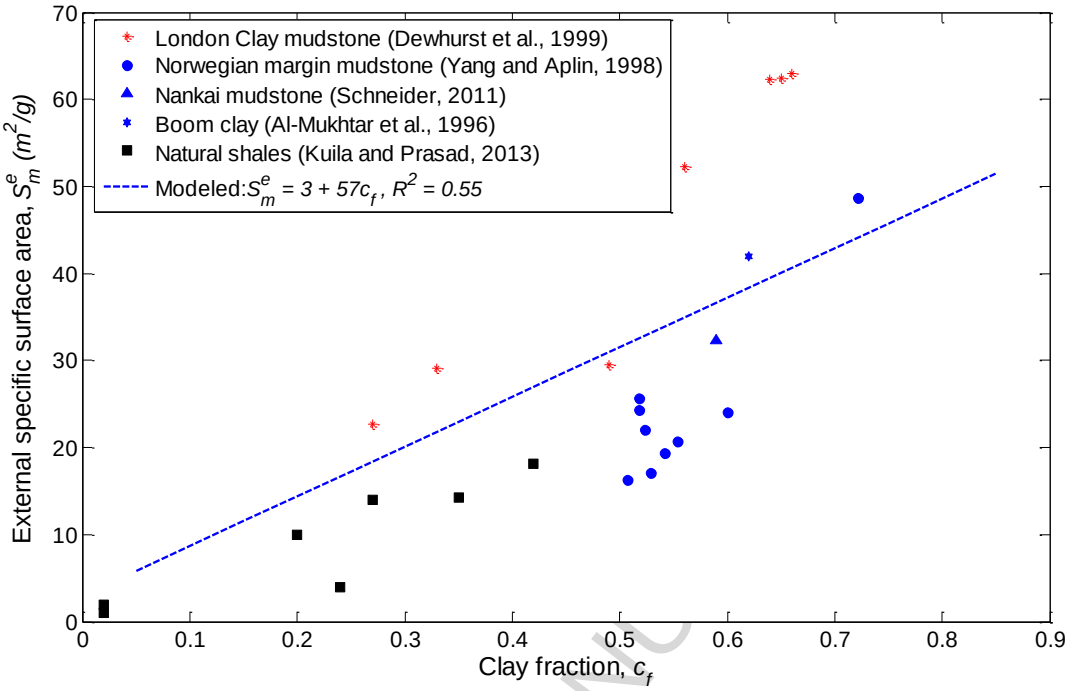

Fig. 17. Measured and modeled relationship between external specific surface area and clay fraction.

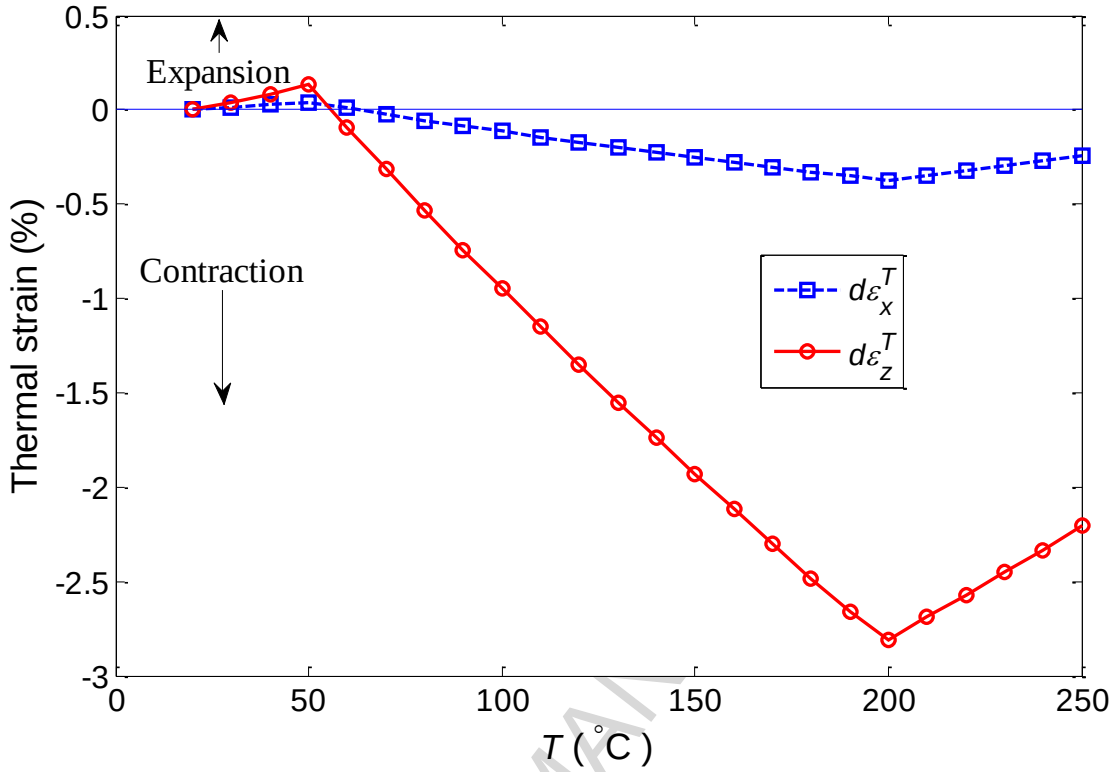

Fig. 18 Estimated thermal contraction strain of sample WCSB1 due to the long term of thermally induced clay dehydration.

Highlights

- A compositional thermal strain model is proposed to investigate the mechanisms of thermally induced deformation in soft mudrocks.
- The model was validated by experimental results on soft mudrock samples with different clay fractions.
- Clay matrix-supported soft mudrocks can have thermal contraction behavior due to clay dehydration or thermal plastic strain.
- The oriented fabric in soft mudrocks contributes to the anisotropy in thermal strains.